Genome sequence and genetic diversity of European ash trees

Elizabeth SA Sollars, Andrea L Harper, Laura J Kelly, Christine Sambles, Ricardo H Ramirez-Gonzalez, David Swarbreck, Gemy Kaithakottil, Endymion D Cooper, Cristobal Uauy, Lenka Havlickova, Gemma Worswick, David J Studholme, Jasmin Zohren, Deborah L Salmon, Bernardo J Clavijo, Yi Li, Zhesi He, Alison Fellgett, Lea Vig McKinney, Lene Rostgaard Nielsen, Gerry C Douglas, Erik Dahl Kjær, J. Allan Downie, David Boshier, Steve Lee, Jo Clark, Murray Grant, Ian Bancroft, Mario Caccamo, Richard JA Buggs

Ash trees (genus *Fraxinus*, Oleaceae) are widespread throughout the Northern Hemisphere, but are being devastated in Europe by the fungus *Hymenoscyphus fraxineus*, causing ash dieback (ADB), and in North America by the Emerald Ash Borer (EAB), *Agrilus planipennis*[1,2]. We sequenced the genome of a low-heterozygosity *Fraxinus excelsior* tree from Britain annotating 38,852 protein-coding genes of which 25% appear ash specific when compared with ten other plant species' genomes. Analyses of paralogous genes suggest a whole-genome duplication shared with olive (*Olea europaea*, Oleaceae). We resequenced 37 *F. excelsior* trees from Europe finding evidence for apparent long-term decline in effective population size. Using our reference sequence, we re-analysed association transcriptomic data[3], yielding improved markers for reduced susceptibility to ADB. Surveys of these markers in British populations suggested that reduced ADB susceptibility may be more widespread in Great Britain than in Denmark. We also present evidence that susceptibility of trees to *H. fraxineus* is associated with their iridoid glycoside levels. This rapid, integrated, multidisciplinary research response to an emerging health threat in a non-model organism opens the way for mitigation of the epidemic.

We sequenced an European ash (*F. excelsior*) tree generated from self-pollination of a woodland tree in Gloucestershire, UK. The sequenced tree (Earth Trust accession 2451S) appeared free of ADB when sampled in 2013 and 2014, but showed symptoms in February 2016. Its genome size was measured by flow cytometry as 877.24 ± 1.41 Mbp. Total genomic DNA was sequenced to 192X coverage (see Supplementary Table 1). We assembled the genome into 89,514 nuclear scaffolds with an N_{50} of 104 kbp, 26 mitochondrial scaffolds, and one plastid chromosome (Supplementary Tables 2-3), where the non-N assembly comprises 80.5% of the predicted genome size. RepeatMasker estimated 35.90% of the assembly to be repetitive elements, with LTR retrotransposons predominating (Supplementary Table 4). In comparison with other eudicot genomes of similar size[4,5] this repeat content is low. The 17% of the assembly comprised of Ns likely contains additional repeats; 27% of reads that do not map to the assembly align to ash repeats (Supplementary Table 5). We generated ~160 million RNA-Seq read pairs from tree 2451S leaf tissue and from leaf, cambium, root, and flower tissue of its parent tree (Supplementary Table 6); low expression of repetitive elements was found in all tissues (Supplementary Table 7).

We annotated the genome using an evidence based workflow incorporating protein and RNA-Seq data, predicting 38,852 protein-coding genes and 50,743 transcripts (Supplementary Table 4). This gene count is within 12% that of tomato (v2.3)[4], potato (v3.4)[6] and hot pepper (v1.5)[7] but higher than monkey flower (v2.0; 26,718 genes)[8]. Evidence for completeness and coherence of our models is shown in Extended Data Fig. 1. Of 38,852 predicted genes 97.67% (and 98.18% of transcripts) were supported by ash RNA-Seq data,

81.80% showed high similarity to plant proteins (> 50% high-scoring segment pair coverage) (Supplementary Table 8), 97.05% had matches in the non-redundant (nr) databases (excluding hits to ash), 82.74% generated hits to InterPro signatures, and 78.09% were assigned Gene Ontology (GO) terms. We also identified 107 microRNA (miRNA), 792 tRNA and 51 rRNA genes.

Past whole genome duplication (WGD) events are commonly inferred from the distributions of pairwise synonymous site divergence (Ks) within paralogous gene groups[9]. We plotted these for ash and six other plant species (Fig. 1a, Supplementary Table 9). Ash and olive shared a peak near Ks = 0.25, suggesting an Oleaceae-specific WGD. A peak near Ks = 0.6 shared by ash, olive, monkey flower and tomato but not by bladderwort, coffee and grape does not fit a common origin hypothesis, unless bladderwort has an accelerated substitution rate and the tomato peak is not restricted to the Solanales as evidenced previously[4]. Synteny analysis between ash and monkey flower did not provide conclusive evidence for shared WGD (Extended Data Fig. 2). Duplicated genes in the ash genome that were not locally duplicated (i.e. within 10 genes of each other in our assembly) show no significantly enriched GO terms at an FDR level of 0.05. In contrast 1,005 locally duplicated genes showed significant enrichment of terms relating to oxidoreductase, catalytic and monooxygenase activity compared to all other genes, suggesting evolution of secondary metabolism by local duplications.

We analysed gene families shared between ash and 10 other species (Supplementary Table 10). In total, 279,603 proteins (77.14% of the input sequences) clustered into 27,222 groups, of which 4,292 contained sequences from all species, 3,266 were angiosperm-specific and 462 Eudicot-specific. Patterns of gene-family sharing among Asterids and among woody species are shown in Figures 1b and c. For 38,852 ash proteins, 30,802 clustered into 14,099 groups, of which 643 were ash-specific, containing 1,554 proteins. There were also 8,050 singleton proteins unique to ash. Of the 9,604 ash-specific proteins, 6,405 matched $\geq$1 InterPro signature. The 20 largest groups in ash are listed in Extended Data Table 1: several are putatively associated with disease resistance.

To investigate genomic diversity in *F. excelsior*, we sequenced 37 ash trees from central, northern and western Europe (Fig. 2 and Supplementary Table 11), to an average of 8.4X genome coverage by trimmed and filtered reads. Together with reads from Danish 'Tree35' (http://oadb.tsl.ac.uk/), these were mapped to the reference genome. We found 12.48M polymorphic sites with a variant of high confidence in at least one individual (qual > 300 using FreeBayes[10]): we refer to these as the 'genome-wide SNP set' in the 'European Diversity Panel'. Of these, 6.85M (54.88%) occur inside or within 5kbp of genes (Supplementary Table 12). We found 259,946 amino-acid substitutions and 71,513 variants that affect stop or start codons, or splice sites. We selected 23 amino-acid variants, and 26 non-coding variants with a range of call qualities for validation using KASP: individual genotype calls with quality > 300 have a false positive rate of 6% and those with quality > 1000 have a false positive rate of zero (Supplementary Table 13). We ran a more stringent variant calling restricted to regions of the genome with between 5 and 30X coverage in all 38 samples. These totalled 20.6 Mbp (2.3% of the genome), within which 529,812 variants were called with CLC Genomics Workbench. Of these, 394,885 were biallelic SNPs with minimum allele frequency above 0.05, which we refer to as the 'reduced SNP set'. We also found c. 31,300 singleton simple sequence repeat (SSR) loci in the ash genome, and designed primers for 664 (Supplementary Data 1). In a sample of 366 of these, 48% were polymorphic in the European Diversity Panel sequences. We PCR tested 48 of these in multiplexes with European Diversity Panel genomic DNA and found that 41 amplified successfully (Supplementary Data 1).

We analysed population structure of the European Diversity Panel using: a plastid haplotype network, STRUCTURE[11] runs on genomic SNPs and principal components analysis of the 'reduced SNP set' (Fig. 2a-d, Extended Data Fig. 3). Clearest differentiation was found in the plastid network, with four distinct haplotype groups each separated from each other by at least 20 substitutions. One group was more frequent in Great Britain than on the continent. The second and third principal components of the PCA corresponded with the plastid data somewhat (Fig. 2c). Previous analyses of SSRs in plastids identified variants unique to the British Isles and Iberia[12]. Linkage disequilibrium (LD) in the European Diversity Panel decayed logarithmically, with an average r^2 of 0.15 at 100 bp between SNPs, reaching an r^2 0.05 at ~40 kbp (Fig. 2e). This is similar to long-range LD estimates found in *Populus tremuloides*[13]. Apparent long-term effective population size decline of *F. excelsior* in Europe was shown by analyses based on heterozygosity in the reference genome (using PSMC[14], Fig. 2f). Such patterns may also reflect a complex history of population subdivision in ash[15].

We used associative transcriptomics to predict ADB damage in Great Britain. We used the full CDS models from our genome annotation as a mapping reference for previously generated[3] RNA-Seq reads from 182 Danish ash accessions ('Danish Scored Panel') that have been exposed to *H. fraxineus*, and scored for damage (Supplementary Data 2). This yielded 40,133 gene expression markers (GEMs; Supplementary Data 3) and 394,006 SNPs (Supplementary Data 4). Twenty GEMs were associated with ADB damage scores, including eight MADS-box proteins, and two cinnamoyl-CoA reductase 2 genes that may be involved in the hypersensitive response (Supplementary Data 5). Four assays representing the top five GEMs were applied to 58 Danish accessions ('Danish Test Panel') to validate the top markers. Results were combined into a single predicted damage score for each tree (Supplementary Data 6), which was compared to the observed damage scores (Fig. 3; R^2=0.25, P=6.9 × 10^{-5}): predictions of damage < 50% consistently detected trees with very low observed damage scores. The same assays were also applied to 130 accessions from across the British range of *F. excelsior* ("British Screening Panel"; Supplementary Data 6). Strikingly, this provided lower predictions for ADB damage in the British Screening Panel: 25% were predicted to have <25% canopy damage, compared to 9% of the Danish Test Panel. Trees with low predicted damage are scattered throughout Britain (Fig. 3).

We also examined expression of the top five GEM loci using RPKM values from our shotgun Illumina read data for the reference tree (Extended Data Fig. 4), comparing these with RPKM values from the Danish Scoring Panel. Expression patterns in the reference tree were highly correlated with those of the most susceptible Danish quartile (R^2=0.995, p<0.001), but not the least susceptible (p=0.24), consistent with observations that the reference tree is now succumbing to the disease. We correlated the expression of all 20 top GEM markers in leaf, flower, cambium and root transcriptomes of the parent of the reference tree. This revealed that leaf expression levels were positively correlated with those in the cambium (R^2=0.65, p<0.001) and flower (R^2=0.38, p=0.0041), but not with the root (p=0.3594).

We identified putative orthologues of the five GEM loci using our OrthoMCL results (Supplementary Data 5) and BLAST searches of GenBank, and conducted maximum likelihood and Bayesian analyses of relevant hits (Extended Data Fig. 5). FRAEX38873_v2_000173540.4, FRAEX38873_v2_000048340.1 and FRAEX38873_v2_000048360.1 clustered into the SVP/StMADS11 group[16] of type II MADS-box genes. FRAEX38873_v2_000261470.1 and FRAEX38873_v2_000199610.1 clustered into the SOC1/TM3 group of type II MADS-box proteins[16,17]. Both groups have roles in flower development[18–21], and appear to be involved in stress response in *Brassica rapa*[22]. Many genes involved in regulation of flowering time in *A. thaliana* are involved in controlling phenology in perennial trees species[23] and genes belonging to the SVP/StMADS11 clade

have potential roles in growth cessation, bud set and dormancy[23]. In *A. thaliana*, *AGL22/SVP* may be required for age-related resistance (ARR)[24].

One mechanism by which transcriptional cascades, such as those involving MADS box genes, might be involved in tolerance or resistance to pathogens is via modulation of secondary metabolite concentrations. For five high-susceptibility and five low-susceptibility Danish trees, we profiled methanol-extracted leaf samples by liquid chromatography mass spectrometry on a quadrupole time-of-flight mass spectrometer. Partial Least Squares Discriminant Analysis (PLS-DA) clearly discriminated high and low susceptibility trees (Fig. 4a). By using accurate mass to identify the chemical nature of discriminant features, we found greater abundance (Fig. 4b) of iridoid glycosides (for details see Extended Data Figures 6-9, and Supplementary Data 9) in high ADB susceptibility genotypes than in low susceptibility genotypes. A MS/MS fragmentation network identified a number of product ions expected from fragmentation of iridoid glycosides (Fig. 4c). Iridoid glycosides are a well-known anti-herbivore defense mechanism in the Oleaceae[25–27]. They can also enhance fungal growth *in vitro*[28], although their aglycone hydrolysis product formed following tissue damage can also mediate fungal resistance[29]. Our data suggest there may be a trade-off between ADB susceptibility and herbivore susceptibility. This is of particular concern given the threat of the herbivore EAB to ash in both North America[1] and Europe[30] and may hamper efforts to breed trees with low susceptibility to both threats.

Literature cited

1. Poland, T. M. & McCullough, D. G. Emerald ash borer: invasion of the urban forest and the threat to North America's ash resource. *J. For.* **104,** 118–124 (2006).
2. Pautasso, M., Aas, G., Queloz, V. & Holdenrieder, O. European ash (*Fraxinus excelsior*) dieback – A conservation biology challenge. *Biol. Conserv.* **158,** 37–49 (2013).
3. Harper, A. L. *et al.* Molecular markers for tolerance of European ash (*Fraxinus excelsior*) to dieback disease identified using Associative Transcriptomics. *Sci. Rep.* **6,** 19335 (2016).
4. Tomato Genome Consortium. The tomato genome sequence provides insights into fleshy fruit evolution. *Nature* **485,** 635–641 (2012).
5. Ming, R. *et al.* Genome of the long-living sacred lotus (Nelumbo nucifera Gaertn.). *Genome Biol.* **14,** R41 (2013).
6. Potato Genome Sequencing Consortium *et al.* Genome sequence and analysis of the tuber crop potato. *Nature* **475,** 189–195 (2011).
7. Kim, S. *et al.* Genome sequence of the hot pepper provides insights into the evolution of

196 pungency in *Capsicum* species. *Nat. Genet.* **46,** 270–278 (2014).
197 8. Hellsten, U. *et al.* Fine-scale variation in meiotic recombination in *Mimulus* inferred from
198 population shotgun sequencing. *Proc. Natl. Acad. Sci. U. S. A.* **110,** 19478–19482
199 (2013).
200 9. Blanc, G. & Wolfe, K. H. Widespread paleopolyploidy in model plant species inferred
201 from age distributions of duplicate genes. *Plant Cell* **16,** 1667–1678 (2004).
202 10. Garrison, E. & Marth, G. Haplotype-based variant detection from short-read sequencing.
203 *arXiv [q-bio.GN]* (2012).
204 11. Pritchard, J. K., Stephens, M. & Donnelly, P. Inference of population structure using
205 multilocus genotype data. *Genetics* **155,** 945–959 (2000).
206 12. Heuertz, M. *et al.* Chloroplast DNA phylogeography of European ashes, *Fraxinus* sp.
207 (Oleaceae): roles of hybridization and life history traits. *Mol. Ecol.* **15,** 2131–2140
208 (2006).
209 13. Wang, J., Street, N. R., Scofield, D. G. & Ingvarsson, P. K. Natural Selection and
210 Recombination Rate Variation Shape Nucleotide Polymorphism Across the Genomes of
211 Three Related *Populus* Species. *Genetics* **202,** 1185–1200 (2016).
212 14. Li, H. & Durbin, R. Inference of human population history from individual whole-genome
213 sequences. *Nature* **475,** 493–496 (2011).
214 15. Mazet, O., Rodríguez, W., Grusea, S., Boitard, S. & Chikhi, L. On the importance of
215 being structured: instantaneous coalescence rates and human evolution-lessons for
216 ancestral population size inference? *Heredity* (2015). doi:10.1038/hdy.2015.104
217 16. Smaczniak, C., Immink, R. G. H., Angenent, G. C. & Kaufmann, K. Developmental and
218 evolutionary diversity of plant MADS-domain factors: insights from recent studies.
219 *Development* **139,** 3081–3098 (2012).
220 17. Wells, C. E., Vendramin, E., Jimenez Tarodo, S., Verde, I. & Bielenberg, D. G. A
221 genome-wide analysis of MADS-box genes in peach [*Prunus persica* (L.) Batsch]. *BMC*
222 *Plant Biol.* **15,** 41 (2015).

18. Liu, C. *et al.* Direct interaction of AGL24 and SOC1 integrates flowering signals in *Arabidopsis*. *Development* **135,** 1481–1491 (2008).
19. Li, D. *et al.* A repressor complex governs the integration of flowering signals in *Arabidopsis*. *Dev. Cell* **15,** 110–120 (2008).
20. Dorca-Fornell, C. *et al.* The *Arabidopsis* SOC1-like genes AGL42, AGL71 and AGL72 promote flowering in the shoot apical and axillary meristems. *Plant J.* **67,** 1006–1017 (2011).
21. Gregis, V., Sessa, A., Colombo, L. & Kater, M. M. AGAMOUS-LIKE24 and SHORT VEGETATIVE PHASE determine floral meristem identity in *Arabidopsis*. *Plant J.* **56,** 891–902 (2008).
22. Saha, G. *et al.* Genome-wide identification and characterization of MADS-box family genes related to organ development and stress resistance in *Brassica rapa*. *BMC Genomics* **16,** 178 (2015).
23. Ding, J. & Nilsson, O. Molecular regulation of phenology in trees — because the seasons they are a-changin'. *Curr. Opin. Plant Biol.* **29,** 73–79 (2016/2).
24. Wilson, D. C., Carella, P., Isaacs, M. & Cameron, R. K. The floral transition is not the developmental switch that confers competence for the *Arabidopsis* age-related resistance response to *Pseudomonas syringae* pv. *tomato*. *Plant Mol. Biol.* **83,** 235–246 (2013).
25. Jensen, S. R., Franzyk, H. & Wallander, E. Chemotaxonomy of the Oleaceae: iridoids as taxonomic markers. *Phytochemistry* **60,** 213–231 (2002).
26. Kubo, I., Matsumoto, A. & Takase, I. A multichemical defense mechanism of bitter olive *Olea europaea* (Oleaceae) : Is oleuropein a phytoalexin precursor? *J. Chem. Ecol.* **11,** 251–263 (1985).
27. Eyles, A. *et al.* Comparative phloem chemistry of Manchurian (*Fraxinus mandshurica*) and two North American ash species (*Fraxinus americana* and *Fraxinus pennsylvanica*). *J. Chem. Ecol.* **33,** 1430–1448 (2007).

28. Marak, H. B., Biere, A. & Van Damme, J. M. M. Systemic, genotype-specific induction of two herbivore-deterrent iridoid glycosides in *Plantago lanceolata* L. in response to fungal infection by *Diaporthe adunca* (Rob.) Niessel. *J. Chem. Ecol.* **28,** 2429–2448 (2002).
29. Biere, A., Marak, H. B. & van Damme, J. M. M. Plant chemical defense against herbivores and pathogens: generalized defense or trade-offs? *Oecologia* **140,** 430–441 (2004).
30. Valenta, V., Moser, D., Kuttner, M., Peterseil, J. & Essl, F. A High-Resolution Map of Emerald Ash Borer Invasion Risk for Southern Central Europe. *For. Trees Livelihoods* **6,** 3075–3086 (2015).

Figure Legends

Figure 1 | Gene sharing within and among plant genomes. a, Distribution of Ks values between paralogous gene pairs within the genomes of ash (*Fraxinus excelsior*), tomato (*Solanum lycopersicum*), coffee (*Coffea canephora*), bladderwort (*Utricularia gibba*), grape (*Vitis vinifera*) and monkey flower (*Mimulus guttatus*), and transcriptome of olive (*Olea europaea*). **b,** Venn diagram of gene sharing by five Asterid species. **c,** Venn diagram of gene sharing by six woody species. Numbers in parentheses are the total number of OrthoMCL groups found for that species; numbers in intersections show the total number of groups shared between given combinations of taxa.

Figure 2 | Genome diversity of *F. excelsior* in Europe. a, Map showing the distribution of plastid haplotypes (n=37), based on a median-joining plastid haplotype network for the European Diversity Panel (inset). **b,** Map showing diversity structure of genomic SNPs, based on average Q-value for each individual (inset), from three runs of STRUCTURE with different sets of 8,955 SNPs and k=3. **c,** Principal component analysis of 34,607 nuclear SNPs in the European Diversity Panel, PC2 plotted against PC3, with points coloured by plastid haplotype. **d,** From the same PCA, PC1 plotted against PC2, with points coloured by groupings found by STRUCTURE using genomic SNPs. **e,** Linkage disequilibrium decay between SNPs in the European Diversity Panel. **f,** Effective population size history estimated using the PSMC method on the reference genome, with 100 bootstraps (shown in light blue).

Figure 3 | Predicted ash dieback damage scores in Britain and Denmark. Map points are scaled by hue (high predicted damage scores in brown, low in green) and plotted according to the geographical origin of the parent trees of the British Screening Panel (n=130) and the Danish Test Panel (n=58). Single leaf samples taken from grafts of each individual tree were used for predicting damage scores. Inset: Damage predictions for the Danish Test Panel (n=58) correlated with log mean observed damage scores from 2013-14 (R^2=0.25, P=6.9 × 10^{-5}).

Figure 4 | Putative iridoid glycosides as discriminatory features between *F. excelsior* genotypes with differential susceptibility to ADB. a, Multivariate analysis PLS-DA score plot of metabolic profiles of five high and five low susceptibility trees (n=3 per genotype). **b,**

Boxplots from these profiles showing normalised (internal standard) intensity (log2 transformed) of five discriminatory features observed in negative mode; m/z and retention time (RT) are given for each feature. **c,** Fragmentation network of discriminatory features, highlighted in black (positive mode) and grey (negative mode). Each product ion is labelled with its size (m/z), also depicted by its circle size. Blue shading increases with the number of times each ion is present in the precursor discriminatory features. Product ions not shared among precursors are shown as unlabelled tips. The edges are in shades of red based on retention time; the paler the colour the earlier the retention time. Those fragment masses shaded in green have been previously reported from fragmentation of iridoid glycosides.

Methods

Tree Material

Reference tree: In 2013 twig material was collected from tree 2451S growing at Paradise Wood, Earth Trust, Oxfordshire. This tree was produced via self pollination of an hermaphroditic *F. excelsior* tree growing in woodland in Gloucestershire (Lat. 52.020592, Long. -1.832804), UK, in 2002 as part of the FRAXIGEN project[31]. The parent tree was one of 19 trees that produced seed from self-pollination, and had lower heterozygosity at four microsatellite loci than the other 18 trees (D. Boshier, unpubl. data). DNA was extracted from bud, cambial and wood tissues using CTAB[32] and Qiagen DNeasy protocols. RNA was extracted using the Qiagen RNeasy protocol from leaf tissue of tree 2451S and from leaf, cambium, root, and flower tissue of its parent tree in Gloucestershire.

European Diversity Panel: In 2014, twig material was collected from 37 trees representing 37 European provenances in a trial of *F. excelsior* established in 2004 at Paradise Wood, Earth Trust, Oxfordshire, UK, as part of the Realising Ash's Potential project. DNA was extracted from cambial tissue of the twigs using a CTAB protocol.

British Screening Panel: In 2015, freshly flushed leaf material was collected from a clonal seed orchard of *F. excelsior* growing at Paradise Wood, Earth Trust, Oxfordshire, UK for RNA extraction and cDNA synthesis as in Harper et al.[3]. Single whole leaves were harvested from four ramets of each of 130 ash trees selected from phenotypically superior parents throughout Britain, that had been cloned by grafting.

2451S DNA Sequencing and Genome Assembly

The genome size of 2451S was estimated by flow cytometry with propidium iodide (PI) staining of nuclei, using leaf tissue co-chopped with an internal standard using a razor blade. Three preparations were made, two with *Petroselinum crispum* 'Curled Moss' parsley as standard (2C = 4.50 pg)[33] and one with *Solanum lycopersicum* 'Stupicke polnı rane' (2C = 1.96 pg)[34] as standard. The Partec CyStain Absolut P protocol was used (Partec GmbH, Germany). Each preparation was measured six times, with the relative fluorescence of over 5000 particles per replicate recorded on a Partec Cyflow SL3 (Partec GmbH, Germany) flow cytometer fitted with a 100-mW green solid state laser (Cobolt Samba; Cobolt, Sweden). The resulting histograms were analysed with the Flow-Max software (v. 2.4, Partec GmbH). The measurement with the tomato internal standard was used as the best estimate of genome size, because the tomato genome size is closest to that of 2451S, yielding a more accurate result.

Genomic DNA of 2451S was sequenced using the following methods: (1) HiSeq 2000 (Illumina, San Diego, CA) at Eurofins, Ebersberg, Germany, with 100 bp reads and shotgun libraries with fragment sizes of 200 bp, 300 bp, and 500 bp, and long jumping distance (LJD) libraries with 3 kbp, 8 kbp, 20 kbp and 40 kbp insert sizes, generating 188X genome coverage; (2) 454 FLX+ (Roche, Switzerland) at Eurofins with shotgun libraries and maximum read length of 1,763 bp and mean length of 642 bp giving 4.3X genome coverage; and (3) MiSeq (Illumina, San Diego, CA) at The Genome Analysis Centre, Norwich, UK, with 300 bp paired-end reads from a Nextera library with ~5 kbp insert size, giving 16X genome coverage (see Supplementary Table 1). We assembled and released five genome assembly versions over the course of 3 years, details of which can be found in Supplementary Table 3. The most recent version assembled first into 235,463 contigs with a total size of 663 Mbp and an N50 of 5.7 kbp (Supplementary Table 2), and after scaffolding and removing organellar scaffolds, the assembly comprised 89,487 scaffolds totaling 867 Mbp (17% "N") with an N50 of 104 kbp (Supplementary Table 2). The plastid genome was assembled separately into one circular contig of 155,498 bp, including an inverted repeat region of approximately 25,700 bp. The mitochondrial genome initially assembled into 296 contigs totaling 232 kbp. After several rounds of contig extension using overlaps of mapped 454 reads the final assembly consisted of 26 contigs totaling 581 kbp with an N50 of 60.6 kbp.

All Illumina reads from 2451S were trimmed using CLC Genomics Workbench (QIAGEN Aarhus, Denmark) versions 6-8 (depending on when the data was received) to a minimum quality score of 0.01 (equivalent to Phred quality score of 20), a minimum length of 50 bp, and were also trimmed of any adaptor and repetitive telomere sequences. The MiSeq Nextera reads were also run through FLASH[35] to merge overlapping paired reads, and NextClip[36] to remove adaptor sequences, both used with default parameters. Roche 454 reads were trimmed to a minimum Phred score of 0.05, and minimum length of 50 bp. *De novo* assembly was performed with the CLC Genomics Workbench, using the 200 bp, 300 bp, 500 bp, and 5 kbp insert size Illumina library reads to build the De Bruijn graphs. The remaining Illumina reads and the 454 reads were used as 'guidance only reads' to help select the most supported path through the De Bruijn graphs. A word size (k-mer) of 50 and maximum bubble size of 5000 were used to assemble the reads into contigs with a minimum length of 500 bp. Contigs were then scaffolded with the stand-alone tool SSPACE[37] Basic v2.0 using all paired Illumina reads, with the '-k' parameter (number of mapped paired reads required to join contigs) set to 7. Gaps in the scaffolds were closed using the GapCloser v1.12 program using all paired reads (except for LJD libraries), with pair_num_cutoff parameter set at 7. 454 reads were mapped to the assembly and used to join overlapping scaffolds using the Jelly.py script from PBSuite[38] v14.7.14 with blasr parameters: -minMatch 11 -minPctIdentity 70 -bestn 1 -nCandidates 10 -maxScore -500 -noSplitSubreads. Contig57544 was removed from the assembly because it aligned fully to the PhiX bacteriophage genome, indicating it derived from the PhiX control library added to Illumina sequencing runs.

To assemble the plastid and mitochondrial genomes, high read depth 50 bp k-mers were extracted from the 200, 300, and 500 bp read libraries. Jellyfish[39] v2.1.1 was used to count the depth for each k-mer, and these values were plotted in a scatterplot to identify peaks that could correspond to the organellar genomes. Every k-mer over 600x coverage was used in a BLAST search against the NCBI non-redundant (nr) database with a filter allowing only plant sequences. K-mers were then extracted based on whether their first hit contained a 'mitochondrion' or 'plastid / chloroplast' related description. Reads from the 200, 300 and 500 bp libraries were then filtered against the k-mer sets, and were kept if the first and last 50 bp matched k-mers from the extracted sets (reads were at most 90 bp long). Each set of reads (mitochondrial and plastid) were then assembled *de novo* using the CLC Genomics Workbench. The plastid genome assembled initially into two contigs, which were joined

using an alignment to the *Olea europaea* plastid genome (GenBank accession NC_015401.1), with the inverted repeat region being identified also. Reads from the 454 library were mapped to the assembly to check the sequence and especially the join region. The mitochondrial genome assembled first into 296 contigs. To fill in gaps and join the contigs together, 454 reads were mapped against the assembly and contig ends were extended using the Extend Contigs tool in the CLC Genome Finishing Module. The Join Contigs tool was then used to join overlapping ends together, and 454 reads were mapped to the resulting assembly to check any joined regions. Using this method of "Map-Extend-Join" iteratively (approximately ten times in total), a more contiguous assembly of 26 contigs was obtained.

RNA Sequencing

The five RNA samples (see "Tree Material" above) were sequenced paired-end on Illumina HiSeq 2000 with 200 bp insert sizes, and a read length of 100 bp at the QMUL Genome Centre, London, UK. Reads were trimmed using CLC Genomics Workbench to a minimum quality score of 0.01 (equivalent to Phred score of 20) and minimum length of 50 bp, and adaptors were also removed (Supplementary Table 6).

Analysis of repetitive DNA

The repetitive element (transposable elements, TEs, and tandem repeats) content of the ash genome was analysed via two approaches: (1) *de novo* identification of the most abundant repeat families from unassembled 454 and Illumina reads; (2) *de novo* and similarity-based identification of repeats from the ash genome assembly.

De novo identification of repeat families from unassembled reads. Individual 454 reads and Illumina read pairs from the 500 bp insert library (post adaptor trimming, but prior to any further quality control or filtering – see above) were used for *de novo* repeat identification. Reads were quality filtered and trimmed using the FASTX-Toolkit v. 0.0.13 (http://hannonlab.cshl.edu/fastx_toolkit/index.html). Using fastx_trimmer, the first 10 bp of all reads (454 and Illumina) was removed (due to skewed base composition). 454 reads were clipped to a maximum of 250 bp and Illumina reads to a maximum of 90 bp; all shorter reads were removed using a custom Perl script. Reads were then quality filtered with the fastq_quality_filter tool to retain only those where 90% of bases had a phred score of ≥ 20. Exact duplicates (which are likely artifacts from the emulsion PCR[40]) were removed from the 454 reads using the fastx_collapser tool.

The complete set of quality filtered and trimmed 454 reads (3,330,483) was used as input for the RepeatExplorer pipeline on Galaxy[41], with a minimum of 138 bp overlap for clustering and a minimum of 100 bp overlap for assembly. All clusters containing ≥ 0.01% of the input reads were examined manually in order to identify clusters that required merging (i.e. where there was evidence that a single repeat family had been split over multiple clusters). Clusters were merged if they met the following three criteria: (1) they shared a significant number of similarity hits (e.g. in a pair of clusters, 10% of the reads in the smaller cluster had BLAST hits to reads in the larger cluster); (2) they were the same repeat type (e.g. LINEs); (3) they could be merged in a logical position (e.g. for repetitive elements containing conserved domains these domains would be joined in the correct order). The re-clustering pipeline was run with a minimum of 100 bp overlap for assembly; merged clusters were examined manually to verify that all domains were in the correct orientation.

Quality filtered and trimmed Illumina reads were paired using the FASTA interlacer tool (v. 1.0.0) in RepeatExplorer, resulting in 111,230,011 pairs; unpaired reads were discarded. An

initial run of RepeatExplorer with a sample of 100,000 read pairs was performed to obtain an estimate of the maximum number of reads that could be handled by the pipeline. A random sample of 3.5 million read pairs was then taken using the sequence sampling tool (v. 1.0.0) in RepeatExplorer and used as input for the clustering pipeline, which further randomly subsampled the reads down to 3,370,186 pairs. The pipeline was run with a minimum of 50 bp overlap for clustering and a minimum of 36 bp overlap for assembly. Clusters containing ≥ 0.01% of the input reads were merged if $k_{x,y}$ passed the 0.2 cut-off (for clusters x and y, $k_{x,y}$ is defined as: $k_{1,2}=2*W/(n_1+n_2)$ where W is the number of read pairs shared between clusters x and y and n_x is the number of reads in cluster x which does not include the other read from its pair within the same cluster); clusters that passed this threshold but which had no similarity hits to each other were not merged. The re-clustering pipeline was run with a minimum of 36 bp overlap for assembly.

Repeat families identified by RepeatExplorer were annotated according to the results of BLAST searches to the Viridiplantae RepeatMasker library, to a database of conserved protein coding domains from transposable elements and to a custom RepeatMasker library comprising all *Fraxinus* sequences (excluding shotgun sequences), all mitochondrial genome sequences from Asterids and all plastid genome sequence from Oleaceae available from NCBI (downloaded on 13.02.2014); these BLAST searches were performed as part of the RepeatExplorer pipeline. For repeat families that were not annotated in RepeatExplorer (i.e. no significant BLAST hits), or where only very few reads (< 2%) had a BLAST hit or separate reads matched different repeat types (i.e. inconsistent BLAST hits), contigs were also searched against the nr/nt database in GenBank using BLASTN with an E-value cut-off[42] of 1e-10, against the nr database using BLASTX with an E-value cut-off of 1e-05, and submitted to Tandem Repeat Finder v. 4.07b with default parameters[43]. Annotation of repeat families from the clustering of the 454 and Illumina data was cross-validated by BLAST searching the contigs from each analysis against each other using the blastn program in the BLAST+ package (v. 2.2.28+) with an E-value cut-off of 1e-10 and the DUST filter switched off. Any repeat families annotated as plastid or mitochondrial DNA were removed prior to downstream analyses (see below).

Identification of repeats from the genome assembly. *De novo* identification of repetitive elements from the assembled ash genome sequence was conducted with RepeatModeler v. 1.0.7 (www.repeatmasker.org/RepeatModeler.html) using RMBlast as the search engine. All unannotated ('unknown') repeat families from the RepeatModeler library were searched against a custom BLAST database of organellar genomes (see above) using BLASTN with an E-value cutoff of 1e-10 in the BLAST+ package (v. 2.2.28+[44]). Any repeat families matching plastid or mitochondrial DNA were removed.

To prevent any captured gene fragments within repetitive element families causing the masking of protein coding genes within the ash assembly, the custom repeat libraries were pre-masked using the TAIR10 CDS dataset[45] (TAIR10_cds_20101214_updated; downloaded from www.arabidopsis.org). First, transposonPSI v2 (http://transposonpsi.sourceforge.net) was run with the 'nuc' option to identify any TE-related genes within the TAIR10 CDS dataset. Sequences with a significant hit to TE-related sequences (E-value cut-off of 1e-05) were removed from the TAIR10 CDS file (n=308); a further 19 sequences that included the term "transposon" in their annotation, but which did not have a hit using transposonPSI, were also removed. The filtered TAIR10 CDS dataset was used to hard mask the RepeatModeler library, the RepeatExplorer libraries (454 and Illumina) and the library from RepeatMasker using RepeatMasker v. 4.0.5 (www.repeatmasker.org) with RMblast as the search engine and the following parameter settings: -s –no_is –nolow. The four pre-masked libraries were combined into a single custom repeat library; any repeat families annotated as 'rRNA', 'low-complexity' or 'simple'

were removed prior to combining the libraries. The combined library was then used to identify repetitive elements in the ash genome assembly with RepeatMasker v. 4.0.5, using the same parameter settings as above. RepeatMasker results were summarised using ProcessRepeats with the species set to 'eudicotyledons' and using the 'nolow' option.

In addition to the analysis with the combined custom ash repeat library, repeats within the assembly were also annotated by running RepeatMasker separately with each of the four individual repeat libraries with parameter settings as described above. The results were saved in gff format and combined into a single gff file that was then used to inform the process of annotating protein coding genes (see below, "Gene Annotation").

Although the ash genome assembly covers c. 99% of the expected genome size based on flow cytometry, c. 17% is comprised of Ns. Therefore, the repeat content of the genome assembly may be an underestimate of the actual amount of repetitive DNA within the genome. To test whether the c. 18% of missing sequence includes additional repetitive elements we analysed the repeat content of individual Illumina reads that do not map to the genome assembly. Quality-trimmed and length-filtered reads from the Illumina short insert libraries (Supplementary Table 1) were mapped to the assembly using the 'Map Reads to Reference' tool in the CLC Genomics Workbench, with both similarity match and length match parameters set to 0.90. Unmapped reads from the 200 bp, 300 bp and 500 bp insert libraries (equating to c. 4.8% of all reads from these libraries; see Supplementary Table 1) were searched against the custom library of ash repeats using blastn (see Supplementary Table 5) with an E-value cut-off of 1e-10 and the DUST filter switched off in the BLAST+ package (v. 2.2.29+[44]).

To test for evidence for the expression of TEs, trimmed RNA sequencing reads from five different tissue types (see Supplementary Table 7) were searched against the custom library of ash repeats using blastn as described above for the unmapped DNA sequencing reads.

Gene Annotation

Protein coding genes were predicted using an evidence based annotation workflow incorporating protein, cDNA and RNA-Seq alignments. Protein sequences from nine species *Amborella trichopoda*, *Arabidopsis thaliana*, *Fraxinus pennsylvanica*, *Mimulus guttatus*, *Populus trichocarpa*, *Solanum lycopersicum*, *Solanum tuberosum*, *Vitis vinifera* and *Pinus taeda* (Supplementary Table 8) were soft masked for low complexity (segmasker-blast-2.2.30) and aligned to the softmasked (for repeats) BATG-0.5 assembly with exonerate[46] protein2genome v-2.2.0 ; alignments were filtered at a minimum 60% identity and 60% coverage, except for *F. pennsylvanica* which were filtered at a minimum of 80% identity and 60% coverage. Publically available *F. excelsior* ESTs (12,083 from Genbank) were aligned with GMAP (r20141229)[47] and filtered at a minimum 95% identity and 80% coverage.

RNA-Seq reads from the five sequenced RNA samples were filtered for adaptors and quality trimmed, rRNA reads were identified and removed[48] (trim_galore-0.3.3 http://www.bioinformatics.babraham.ac.uk/projects/trim_galore/ : -q 20 --stringency 5 --length 60; sortmerna-1.9: -r 0.25 --paired-out). RNA-Seq reads were aligned using Tophat (v2.0.13/bowtie-2.2.3)[49] and transcript assemblies were generated using three alternative methods Cufflinks (v2.2.1)[50], StringTie (v1.04)[51] and Trinity (genome guided assembly) [52]. Assembled Trinity transcripts were mapped to the *F. excelsior* assembly using GMAP (r20141229) at 80% coverage and 95% identity. A comprehensive transcriptome assembly was created using Mikado (v0.8.5 – in-house tool, manuscript in preparation) based on the GMAP Trinity alignments, Cufflinks and StringTie transcript assemblies. Mikado leverages transcript assemblies generated by multiple methods to improve transcript reconstruction.

Loci are first defined across all input assemblies with each assembled transcript scored based on metrics relating to ORF and cDNA size, relative position of the ORF within the transcript, UTR length and presence of multiple ORFs. The best scoring transcript assembly is then returned along with additional transcripts (splice variants) compatible with the representative transcript.

Protein coding genes were predicted using AUGUSTUS[53] by means of a Generalized Hidden Markov Model (GHMM) that takes both intrinsic and extrinsic information into account. An AUGUSTUS *ab initio* model was generated based on a subset of cufflinks assembled transcripts identified by similarity support as containing full-length open reading frames. Gene models were predicted using the trained *ab initio* model with the nine sets of cross species protein alignments, RNA-Seq junctions (defining introns), and Mikado transcripts as evidence hints. RNA-Seq read density was provided as exon hints and repeat information (interspersed repeats) as nonexonpart hints. We generated two alternative AUGUSTUS models by either including or excluding the RNA-Seq read depth information. A set of integrated gene models was derived from the two AUGUSTUS runs along with the transcriptome and protein alignments via EVidenceModeler:r20120625 (EVM)[54]. Weights of evidence were manually set following an initial testing and review process as: AUGUSTUS predictions with RNA-Seq read depth hint, weight 2; AUGUSTUS predictions without RNA-Seq read depth hint, weight 1; protein alignment high confidence (greater than 90% coverage, 60% identity) weight 5; protein alignment low confidence (lower than 90% coverage 60% identity) weight 1; cufflinks transcripts, weight 1; Mikado transcripts, weight 10; RNA-seq splice junctions, weight 1. We identified examples of EVM errors resulting from incomplete genes in the AUGUSTUS gene predictions or non-canonical splicing; to rectify these problems we substituted the EVM model for the overlapping AUGUSTUS model (with RNA-Seq read depth hints). To add UTR features and alternative splice variants we ran PASA [55] with Mikado transcript assemblies and available *F. excelsior* ESTs using the corrected EVM models as the reference annotation.

The PASA updated EVM models were further refined by removing gene models that showed no expression support (using all available RNA-Seq libraries) or had no support from cross species protein alignments or no blast similarity support with a Viridiplantae (without *Fraxinus excelsior)* protein database (< 50% blast high-scoring segment pair (HSP) coverage) or where the CDS length was less than 100 bp (retaining those transcripts with ≥ 50% blast HSP coverage). Gene models were also excluded if they aligned with ≥ 30% similarity and 40% coverage to the TransposonPSI (v08222010) library (http://transposonpsi.sourceforge.net/) and had ≥ 40% coverage by the RepeatModeler/RepeatMasker derived interspersed repeats. In addition, gene models that had ≥ 30% similarity and 60% coverage to the TransposonPSI library or had ≥ 60% coverage by the RepeatModeler/RepeatMasker derived interspersed repeats were also excluded. The functional annotation of protein coding genes was generated using an in-house pipeline - AnnotF-1.01, that executes and integrates the results from InterProSCAN (version 5) and Blast2GO (version 2.5.0). Completeness of transcript models was classified by Full-lengther Next[56] and coherence in gene length examined by comparison with single copy gene BLAST hits in monkey flower (Extended Data Fig. 1).

Transfer RNA (tRNA) genes were predicted by tRNAscanSE-1.3.1 with eukaryote parameters[57] and rRNAs using rnammer-1.2[58]. miRNA was predicted by BLASTN searches with precursor miRNAs from miRBase[59] 21.0 against the reference genome sequence (BLAST 2.2.30, E-value 1e-06) and miRCat[60] using the mature miRNAs from miRBase with default plant parameters, except modifying the flanking window to 200 bp. Putative miRNA precursors from these methods were combined and were folded using RNAfold[61] and mature

miRNAs from miRBase were aligned to precursor hairpins using PatMaN[62]. These predictions were checked manually for RNA secondary structure.

Organellar genes were annotated manually using the BLAST tool within the CLC Genomics Workbench v7.5. Mitochondrial genes were identified using CDS from *M. guttatus, Nicotiana tabacum* and *A. thaliana* (all downloaded from NCBI). Plastid genes were identified using CDS from *Olea europaea* and *N. tabacum* (both downloaded from NCBI). An E-value cut-off of 1E-04 was used. Gene and CDS annotations were added manually to the *F. excelsior* organellar scaffolds using the sequence editing tools available within the CLC Genomics Workbench. In the plastid genome, we annotated 72 protein-coding, 7 putative coding (ycf), rRNA, and tRNA genes. On the mitochondrial scaffolds, we annotated 37 protein-coding, rRNA and tRNA genes.

Analysis of whole genome duplications

To examine evidence for past whole genome duplication, CDS and protein sequences (one transcript per gene) were taken from our ash genome annotation, and downloaded from Phytozome v10.3 for tomato (*S. lycopersicum*), monkey flower (*M. guttatus*), and grape (*V. vinifera*), the CoGe database for bladderwort (*Utricularia gibba*) and coffee-genome.org for coffee (*Coffea canephora*). For olive (*Olea europaea*) we predicted open reading frames from transcriptome data[63] using Transdecoder[52] with all parameters set to defaults (v.2.01 http://transdecoder.github.io). Olive[63] is in the same family as ash (Oleaceae); monkey flower[8] and bladderwort[64] in the same order as ash (Lamiales); tomato[4] , and coffee[65], in different orders (Solanales and Gentianales, respectively), but like ash in the Asterids; and grape[66], is a Rosid. An all-against-all comparison using protein sequences was carried out on each species separately using BLASTp v2.2.29, with an e-value cutoff of 1E-05. BLAST alignments were further filtered to retain pairs for which the shorter sequence was at least 50% of the longer sequence, and the alignment was at least 50% of the shorter sequence. If one sequence had multiple matches meeting the length and e-value thresholds these were grouped into a paralog group, including any other genes that were associated with the matches (e.g. if gene A matches gene B and gene C, and gene C also matches gene D, then one group of A, B, C and D would be formed).

Next, all possible pairs of protein sequences within each group were aligned using muscle v3.8.31 with default parameters[67]. A nucleotide alignment was generated from the protein alignment using a python script. Synonymous substitutions were estimated using the codeml program from PAML v4.8[68]. The Ks scores within each group were then corrected to remove redundant values; only those representing duplication events within the group were retained (in a group of n genes, there are n-1 possible duplication events) using the method described in Maere et al[69] and Blanc & Wolfe[9]. These steps are implemented in a python script available online: github.com/EndymionCooper/KSPlotting.

In order to examine patterns of conserved synteny we constructed syntenic dotplots using the SynMap[70] with default parameters (Extended Data Fig. 2). The default uses LAST[71] to perform similarity searches, and DAGchainer[72] to find syntenic regions. By default DAGchainer requires a minimum of five aligned gene pairs with no more than 20 genes between neighbouring pairs.

Pairs of genes were categorised as ‘local’ duplications if they were located on the same chromosome or scaffold and resided within 10 genes of each other, and as ‘tandem’ duplications if they reside directly next to each other. GO term enrichment was performed on ash proteins using the BLAST2GO plugin suite of tools within the CLC Genomics Workbench v8.5. Three separate BLAST searches were run against the RefSeq protein

database: firstly using CDS from all genes as queries, secondly using CDS from genes involved in WGD (excluding locally duplicated genes), and thirdly using CDS from locally duplicated genes (genes located within 10 genes of each other). The E-value cut-off for all BLAST runs was 1e-05. BLAST results were annotated with GO terms using the 'Mapping' and 'Annotation' tools within the BLAST2GO plugin, using default parameters except for: Annotation Cutoff = 55 and HSP-Hit Coverage Cutoff = 40. Significantly enriched GO terms were identified using the Fisher Exact Test tool within the plugin, where the reference set was the GO terms for all genes, and an FDR of 0.05 was used.

Analysis of gene families

The OrthoMCL pipeline (v.2.0.9)[73] was used to identify clusters of orthologous and paralogous genes from *F. excelsior* and: *Amborella*[74], *Arabidopsis*[75], barrel medic[76], bladderwort[64], coffee[65], grape[66], loblolly pine[77], monkey flower[8], poplar[78] and tomato[4] (Supplementary Table 10). Input proteomes contained a single transcript per gene and were filtered with orthomclFilterFasta to remove any sequences of < ten amino acids in length and/or > 20% stop codons. Similar sequences were identified via an all versus all BLASTP search for the 362,741 proteins remaining after filtering. The BLAST search was performed in the BLAST+ package[44] (v.2.2.29+), using an e-value cut-off of 1e-05. BLAST results were filtered with orthomclPairs to retain protein pairs that match across ≥ 50% of the length of the shorter sequence in the pair. Clustering of sequences was carried out with mcl[79] (v.14.137) using a setting of 1.5 for the inflation parameter. The output from OrthoMCL was summarised using a custom Perl script to obtain counts of the number of sequences from each species belonging to each group. Venn diagrams for selected taxa were generated using InteractiVenn[80].

European Diversity Panel sequencing

DNA from the 37 European Diversity Panel trees was sequenced at The Genome Analysis Centre on Illumina HiSeq, using paired-end insert sizes between 100 and 700 bp, and a read length of 150 bp. This generated an average of 63.6 million 150 bp reads (10.9X genome coverage) per tree. Filtering and trimming steps reduced this average to 55.3 million reads. An average of 85.8% of these reads per tree mapped to our reference genome. In addition, DNA reads from Danish Tree35 library '3077' were downloaded from the Open Ash Dieback ftp site (http://oadb.tsl.ac.uk); these were 250 bp paired-end reads with an insert size between 200 and 400 bp. Tree35 is given the sample number '38' in all further population analysis.

European Diversity Panel genome-wide SNP calling

The raw reads from the 37 trees in the European Diversity Panel (Supplementary Table 11) were aligned to the reference genome using bowtie 2.2.5[81]. The alignments were converted to the BAM format and the duplicated reads were removed with samtools 1.2[82]. To assign each read to its corresponding tree, the flag 'rg' was added to each BAM file with picard tools 1.119 (http://broadinstitute.github.io/picard/). SNPs were called with freebayes 1.0.2[10] to produce a VCF file. The SNPs with quality < 300 were filtered with bio-samtools 2.1[83]. SnpEff 4.1g[84] was used to predict the effect of the putative SNPs (see Supplementary Table 12). Genic regions were within 5kbp from a gene model. Amino acid changes are labelled as missense_variant.

SNP calls validation using the KASP platform

In order to test the reliability of SNP calls in the genome-wide SNP calling, we designed KASP assays for 53 SNPS, which ranged in their level of confidence (see Supplementary Table 13). None of the SNP calls tested by KASP were present in the reduced SNP set used for population genetic analyses. Primers were designed with a modified version of PolyMarker[85] including the FAM or HEX tails (FAM tail: 5′ GAAGGTGACCAAGTTCATGCT 3′; HEX tail: 5′ GAAGGTCGGAGTCAACGGATT 3′). The primer mix was prepared as recommended by the manufacturer [46 μL dH2O, 30 μL common primer (100 μM) and 12 μL of each tailed primer (100 μM)] (http://www.lgcgroup.com/services/genotyping). The assays were run on 37 individuals from the European Diversity panel, in 384-well plates as 4μL reactions [2-μL template (10–20 ng of DNA), 1.944 μL of V4 2× Kaspar mix and 0.056 μL primer mix]. PCR was done with the following protocol: hotstart at 95 °C for 15 min, followed by ten touchdown cycles (95 °C for 20 s; touchdown 65 °C, −1 °C per cycle, 25 s) then followed by 30 cycles of amplification (95 °C 10 s; 57 °C 60 s). Fluorescence was detected on a Tecan Safire at ambient temperature. Genotypes were called using Klustercaller software (version 2.22.0.5; LGC Hoddesdon, UK). Four of the individuals did not amplify and were discarded from the analysis. The result of the calls are in Supplementary Data 7.

European Diversity Panel population genetics and history using a reduced set of SNPs

For population structure analyses and effective population size estimation, variants were only called at SNP sites in the genome where all 38 samples have between 5 and 30x coverage. We refer to this as the ‘reduced SNP set’.

First, all reads were trimmed in the CLC Genomics Workbench to a minimum quality score of 0.01 (equivalent to Phred quality score of 20), a minimum length of 50 bp, and were also trimmed of any adaptor and repetitive telomere sequences. Filtered reads were mapped to the reference assembly using the ‘Map Reads to Reference’ tool in the CLC Genomics Workbench, setting both similarity match and length match parameters to 0.95. Regions with coverage of between 5 and 30 reads in all samples were extracted using the ‘Create Mapping Graph’, ‘Identify Graph Threshold Areas’ and ‘Calculus Track’ tools. These extracted regions totaled 20.6 Mbp (2.3% of the genome)

Variant calling was performed on a read mapping pooled from all samples, using the ‘Low Frequency Variant Caller’ tool in the CLC Genomics Workbench, with the coverage-restricted regions from the previous step used as a track of target regions. This prevented variants being called where some samples did not have read coverage, and also in the organellar scaffolds where the read coverage is very high. The following parameters were changed from default: Ignore positions with coverage above = 1000, Ignore broken pairs = no, Ignore non-specific matches = Reads, Minimum Coverage = 190 (38 samples with at least 5 reads each should have a combined total coverage of > 190), Minimum Count = 10, Minimum Frequency = 5%, Base Quality Filter = Yes, Neighbourhood radius = 5, Minimum Central Quality = 20, Minimum neighbourhood quality = 15, Read Direction Filter = yes, Direction Frequency = 5%. As a result 529,812 variants were called, comprising 468,237 SNPs, 14,850 equal replacements (where > 1 nucleotides are replaced by an equal number of nucleotides), 26,043 deletions, 19,085 insertions, and 1,597 unequal replacements (where at least one SNP lies directly beside an indel). The average quality of all reads at these variant positions was 36.2.

To genotype each sample individually at the variant loci called in the previous steps, the ‘Identify Known Mutations from sample mappings’ tool within the CLC Biomedical Genomics workbench was used. The workflow takes a track of known variants as input (such as those called from the pooled read mapping) and reports the presence, absence, coverage, count

and other statistics, of each variant locus in the read mapping of another sample (in this case, the read mapping from each of the 38 trees). The 'Identify Candidate Variants' tool was then used to filter variants with a minimum coverage of 5, minimum count of 3 and minimum frequency of 20%. VCF files for each tree were exported from the CLC Workbench and merged into one file using the vcf-merge tool from VCFtools[86]. The merged VCF file was then filtered using vcftools, to remove indels, multi-allelic loci, and loci with a Minimum Allele Frequency (MAF) < 0.05, with 394,885 SNP loci remaining. This set of high quality SNPs with comprehensive knowledge of the genotype of every sample is referred to as the 'reduced SNP set' and is used for further population analyses.

To visualise similarities and differences among the genomes of the European Diversity Panel, PCA was performed using the SNPRelate v1.4.2[87] package in R v3.1.2. The filtered VCF file was converted into gds using the snpgdsVCF2GDS command, and was filtered on an LD value of 0.1 using the snpgdsLDpruning command, leaving 34,607 SNPs. PCA was performed on the pruned set of SNPs using the snpgdsPCA command with default options, and the results of the first three PCs were plotted in R.

To analyse population structure in the European Diversity Panel, scaffolds were selected that contained 10 or more SNPs in the filtered VCF file (8,955 nuclear scaffolds in total). Three different SNPs were selected at random from each of these scaffolds, and placed into three different files in STRUCTURE input format (26,865 SNPs in total, 8,955 in each set). STRUCTURE v2.3.4[88] was run with admixture from k=1 to k=20 for each of the three sets of SNPs, with both BURNIN and NUMREPS set to 100,000. All output results were run through Structure Harvester Web v0.6.94[89], which found k=3 to have the largest delta k value of 32.91 (Extended Data Fig. 3). Next, the three runs of k=3 were used as input into CLUMPP v1.1.2[90] to align the clusters, and samples within each cluster. Aligned results were imported back into STRUCTURE v2.3.4 to generate Q-value bar plots. Average Q-values from the three runs were used to generate a map with pie charts, using Tableau v9.3 (Tableau, Seattle, US) with Tableau base-map country outlines. Each section of the pie represented the average Q-value of the individual belonging to the coloured cluster (Fig. 2b).

To analyse relationships among plastid sequences in plastid haplotype networks, a consensus sequence of the large single copy plastid region was extracted for each of the 38 samples. The sequences were then aligned using the Create Alignment tool in the CLC Genomics Workbench, and the alignment was exported in Phylip format. The alignment was imported into PopArt v1.7 [http://popart.otago.ac.nz], where a Median-Joining network was generated. Results were visualised on a map using Tableau v9.3 (Fig. 2a) with Tableau base-map country outlines.

We estimate the effective population size history of *F. excelsior* using two complementary methods; the PSMC[14] model estimates the history in the non-recent past, whereas by using Linkage Disequilibrium, we can estimate the population size more recently. The Pairwise Sequentially Markovian Coalescent (PSMC) model calculates the effective population size using a Time to Most Recent Common Ancestor (TMRCA) approach. The effective population size history is then estimated from the number of recombination events separating segments of constant TMRCA. The program PSMC 0.6.5[14], takes only a diploid consensus sequence as input. To estimate past effective population size, PSMC analysis was used on the reference tree. DNA reads from the 2451S 200, 300 and 500 bp libraries were mapped to the 2451S reference sequence using CLC Genomics Workbench 'Map Reads to Reference' tool (length fraction = 0.95 and similarity fraction = 0.9). The mapping was exported in bam format, and a consensus sequence was obtained following PSMC recommendations, by using samtools v0.1.18 'mpileup' command with options: -C 50 -A -Q 20 -u, bcftools v1.1 to convert the bcf file to vcf format, and finally using vcfutils.pl to convert

the vcf file to a consensus sequence where the coverage was between 5 and 200. The PSMC program was then run with default parameters except for: -p "4+25*2+4+6", with one hundred bootstraps. To scale the results, the psmc_plot.pl script was used with default parameters except for the following: -u 7.5e-09 -g 15 -N 0.25 (the mutation rate of *F. excelsior* is unknown, so the substitution rate of 7.5e-09 is taken from a study on *Arabidopsis thaliana*[91]). Effective population size estimates were then plotted in R v3.1.2 (Fig. 2f).

Effective population size estimation by Linkage Disequilibrium (LD) in the European Diversity Panel was performed using the program SNeP v1.1[92], which takes genome-wide polymorphism data from several individuals in a population as input. The European Diversity Panel filtered VCF file with the reduced SNP set of 38 trees (same as used in PCA and STRUCTURE analysis) was converted into Map and Ped files. The third column in the Map file (linkage distance in Morgans) was set to zero for all SNPs, as these values were unknown and SNeP calculates this value from each SNP's physical distance. SNeP was then run with a minimum distance between SNPs of 10,000 bp and a maximum of 400,000 bp, with Sved's modifier for recombination rate, and with 50 bins. Estimated effective population sizes were plotted in R (Extended Data Fig. 3c), as well as LD decay over distance between 100 and 300,000 bp (Fig. 2e).

Simple-sequence repeat analysis

To develop accessible population genetic markers, the repeat masked v0.4 2451S genome was mined for simple sequence repeat (SSR) sequences (a repeat motif of 2-5 bp in length repeated a minimum of 5 times) using the QDD-v.3.1 pipeline[93]. Downstream QDD-v.3.1 pipes screened SSR loci (inclusive of the SSR repeat motif and 200 bp forward and reverse flanking regions) for singleton sequences in an all-against-all BLAST (-task blastn -evalue 1e-40 -lcase_masking -soft_masking true) and designed primer pairs within 200 bp flanking regions using PRIMER3 software[94].The c. 31,300 singleton SSR loci identified in the ash genome were screened using RepeatMasker Open-4.0 (http://www.repeatmasker.org) in QDD-v.3.1 to eliminate loci which hit known transposable elements in the RepBase Viridiplantae repeat library (http://www.girinst.org), leaving c. 28,800 SSR loci. The final primer table output by the QDD-v.3.1pipeline allows selection of the best primer pair design for each SSR loci. To select candidate markers for further development, these primer pairs were filtered according to parameters provided by QDD-v.3.1. The selected SSR loci had a: maximum primer alignment score of 5; minimum 20 bp forward and reverse flanking region between SSR and primer sequences; high quality primer design (defined by QDD pipeline as an absence of homopolymer, nanosatellite, and microsatellite sequence in primer and flanking sequences), and; minimum number of 7 motif repeats within the SSR sequence. This filtering gave a set of 837 SSR loci, which was screened against the combined custom ash repeat library for v0.5 of the 2451S genome assembly (see above - "Analysis of repetitive DNA") via a blastn search with an E-value of 1e-10 in the BLAST+ package (v. 2.2.31+). Elimination of all sequences with a hit to known repetitive elements left 681 candidate loci. These were compared to the v0.5 assembly via a blastn search with an E-value cut-off of 1e-10. This returned a set of 664 loci with a unique match to the v0.5 assembly for use as population genetic markers (see Supplementary Data 1).

In silico analysis of allelic diversity (i.e. locus polymorphism) of these SSR loci was carried out by screening a subset of loci (366) against a variance table composed of insertions and deletions recorded for the European Diversity Panel. Approximately half (48%) of the loci tested were variable among 37 of the resequenced genomes (sample 38 not included). Twenty candidate SSR loci with the greatest *in silico* allelic diversity were selected for wet lab testing on seven individuals from the European Diversity Panel. Primer pairs with a fluorescent tag on the 5' end of the forward primer (FAM, HEX or TAM) were used. For

singleplex PCR, primer aliquots were used at a concentration of 10 pmol/µl . PCR amplification of target regions was carried out in singleplex reactions with a final reaction volume of 10 ul, containing 1 ul genomic DNA, 0.2 ul of each primer (10pmol/ ul), 3 .6 ul of RNAse free water, and 5 ul of Qiagen Type-it Multiplex PCR Master Mix, in a G-Storm GS2 Multi Block Thermal Cycler. The amplification conditions were as follows: 5 min at 95°C; 18 cycles of 30 s at 95 °C, 90 s at 62 °C with a 0.5 °C reduction per cycle, 30 s at 72 °C; 20 cycles of 30 s at 95°C, 1 min 30s at 51 °C, 30 s at 72 °C; a final extension step of 30 min at 60 °C. PCR samples were diluted to 1:10 with dH_20 and run (on an Applied Biosystems 3730xl 96 capillary sequencing instrument with Applied Biosystems GeneScan 400HD Rox dye size standard. Negative control samples were included for each primer pair PCR reaction mix. Allele calling was carried out using GeneMarker v.2.6.4 (http://www.softgenetics.com).

Primer pairs which produced interpretable allele peaks from capillary sequencing of singleplex reactions were arranged into four multiplex primer mixes (containing 5 primer pairs each) according to PCR product size and fluorescent tag. Multiplex primer mixes were tested on DNA extractions for a further 14 of the 37 trees from the European Diversity Panel. For each multiplex, primer pair mixes were prepared at a final concentration of 10pmol/ µl and amplified via PCR in 10µl reaction volumes (1 ul genomic DNA, 1 ul primer mix, 3 ul of RNAse free water, and 5 ul of Qiagen Type-it Multiplex PCR Master Mix) under the amplification conditions described above. PCR product size range, allele counts, primer design and successful multiplex panels for the 20 wet lab tested candidate SSR markers developed for European ash are described in Supplementary Data 1.

Further multiplex primer mixes were tested on 7 trees from the European Diversity Panel for amplification of the longest SSR loci (14 or more repeated motifs). Primer pair mixes were prepared at a final concentration of 10pmol/ul and amplified via PCR in 8µl reaction volumes (1 ul genomic DNA from a 1:10 dilution with nuclease free water, 1 ul primer mix, 2 ul of RNAse free water, and 4 ul of Qiagen Type-it Multiplex PCR Master Mix.). The amplification conditions were as follows: 5 min at 95°C; 32 cycles of 30 s at 95 °C, 90s at 62 °C with a 0.35 °C reduction per cycle, 30 s at 72 °C; a final extension step of 30 min at 60 °C. Amplification was performed in a G-Storm GS2 Multi Block Thermal Cycler. Size fraction analysis of PCR products was carried out for two samples of each tested primer multiplex using a 12 sample DNA1000/7500 chip in an Agilent 2100 Bioanalyzer (http://www.genomics.agilent.com). Of the 28 primer pairs tested, 22 successfully amplified across the six primer multiplexes tested (Supplementary Data 1).

Association of transcriptomic markers with reduced susceptibility to ash dieback in Denmark

Sequence reads for the “Danish Scored Panel” of 182 Danish ash accessions (as described in Harper *et al*., 2016[3]; sequence reads are available in the European Nucleotide Archive under the study accession number PRJEB10202) were mapped to a reference composed of the complete set of CDS models (including 229 genes identified as possible TEs; see above, Gene Annotation). This provided transcript abundance estimates for 40,133 CDS models (Supplementary Data 2). Transcript abundance was quantified and normalized as reads per kbp per million aligned reads (RPKM). After filtering out models exhibiting negligible expression (mean RPKM value of below 0.4), 33,204 CDS models were analysed as potential gene expression markers (GEMs; Supplementary Data 3). SNPs were called by the meta-analysis of alignments (as described in Bancroft *et al*.[95]) of mRNA-seq reads obtained from each of the 182 accessions. SNP positions were excluded if they did not have a read depth in excess of 20, a base call quality above Q20, missing data below 0.25, and three alleles or fewer. An additional noise threshold was employed to reduce the effect of

sequencing errors, whereby ambiguous bases were only allowed to be called if both bases were present at 0.15 or above. This resulted in a final set of 394,006 SNPs (Supplementary Data 4) of which 234,519 had minor allele frequencies in excess of 0.05, and all of which were within the CDS models constituting the GEM panel.

The SNP dataset for the 182 accessions was entered into the program PSIKO[96] to produce a Q matrix, which was composed of two population clusters. The SNP genotypes, Q matrix and ash dieback damage scores for these trees[3] were incorporated into a compressed mixed linear model[97] implemented in the GAPIT R package[98], with missing data imputed to the major allele. The kinship matrix used in this analysis was also generated by GAPIT.

Gene expression marker (GEM) associations were calculated by a fixed effect linear model in R with RPKM values and the Q matrix inferred by PSIKO as the explanatory variables and damage score the response variable. R^2, regression coefficients, constants and significance values were outputted for each regression.

Twenty GEMs were associated with damage scores (Supplementary Data 3). A previous analysis of the gene expression data, based on a simple mRNA transcript reference, identified only 13 GEMs associated with ash dieback damage in ash[3], with the strongest associations exhibiting higher P values than the present study (best P values 5.31×10^{-12} and 9.83×10^{-13} respectively). The CDS models for the top three GEMs identified in the present study had very high BLAST similarity to the transcripts for two of the GEMs identified in the previous study. FRAEX38873_v2_000173540.4 ($P = 1.95 \times 10^{-10}$) corresponds with Gene_23247_Predicted_mRNA_scaffold3380 from the previous study, but Gene_19216_Predicted_mRNA_scaffold2427 resolved into two distinct CDS models in the present study (FRAEX38873_v2_000261470.1, $P = 9.83 \times 10^{-13}$ and FRAEX38873_v2_000199610.1, $P = 6.01 \times 10^{-12}$). The qRT-PCR primers designed for the previous analysis[3] were adequate for assaying FRAEX38873_v2_000173540.4 and FRAEX38873_v2_000261470.1 and new primers were designed for FRAEX38873_v2_000199610.1.

Two of the 20 significantly associated GEMs in the present study, FRAEX38873_v2_000048360.1 ($P = 1.77 \times 10^{-9}$) and FRAEX38873_v2_000048340.1 ($P = 3.48 \times 10^{-7}$), did not have high BLAST similarity to GEMS found in the previous study. However, these GEMs were highly similar to a cDNA transcript containing a predictive A/G SNP (termed a cSNP) identified previously, where presence of a G allele was associated with low damage scores. Both of these GEMS contained the “less susceptible” G variant. A third paralogous gene in this family with the A variant was also found (FRAEX38873_v2_000184430.1), and was not identified as a GEM associated with damage score ($P = 0.02$). The present study therefore resolves this cSNP marker into three paralogous genes, two fixed for a “less susceptible” G nucleotide, and one a “susceptible” A nucleotide.

These five GEMs were applied using qRT-PCR, and in the case of FRAEX38873_v2_000048360.1 and FRAEX38873_v2_000048340.1 RT-PCR, to a small test panel of 58 Danish accessions (henceforth “Danish Test Panel”) to assess their predictive capabilities in a similar way as in Harper et al.[3]. Unlike this previous study however, ratios between the bases of the FRAEX38873_v2_000048360.1 and FRAEX38873_v2_000048340.1 were scored by eye (instead of simply scoring the presence or absence of the “less susceptible” nucleotide), in order to estimate levels of gene expression for the “less susceptible” paralog, whilst maintaining the simplicity of the assay. These ratios and the qRT-PCR assays for the other three GEMs were combined into a single predicted damage score for each of the Danish Test Panel, which could then be

compared with the observed damage scores for these trees. The combined prediction was correlated with the log mean damage scores for 2013-14 (R^2=0.25, P=6.9 × 10^{-5}) which gave a small improvement in predictive power from the previous analysis (R^2=0.24, p<8.4 × 10^{-5}).

Screening of UK *F. excelsior* accessions for markers of reduced susceptibility to ash dieback

Four markers were selected for predictive marker assays based on this analysis and previous work on the Danish Test Panel of 58 trees[3]. The three GEM markers most highly associated with disease damage were assayed by qRT-PCR using the following primer combinations: FRAEX38873_v2_000261470.1 (GTCGAGGAGGATGGTCAGTCAT, AATCTTGCGGAGGACCTATCG), FRAEX38873_v2_000199610.1 (GGTGAGAGGAAAGGTTCAAATGA, TGCGTTTTGAGAAGGAAACCA), FRAEX38873_v2_000173540.4 (AGGGCAAGGCTTGGAAACAT, TAGGCTTTTTTCTAGCTGCTTGTCA) and GAPDH reference (CTGGGATCGCTCTTAGCAAGA, CGATCAAATCAATCACACGAGAA).

Using RNA extracted from the British Screening Panel, qRT-PCR reactions were performed with SYBR Green fluorescence detection in a qPCR thermal cycler (ViiA™ 7, Applied Biosystems, San Francisco, CA) using optical grade 384-well plates, allowing all reactions to be performed simultaneously for each target gene. Each reaction was prepared using 3 µl from a 2 ng/µl dilution of cDNA derived from the RT reaction, 5 µl of SYBR® Green PCR Master Mix (Applied Biosystems®), 200 nM forward and reverse primers, in a total volume of 10 µl. The cycling conditions were: 2 min at 50°C, 10 min at 95°C, followed by 40 cycles of 95°C for 15 sec and 60°C for 1 min with the final dissociation at 95°C for 15 sec, 60°C for 1 min and 95°C for 15 sec. Three technical replicates were used for quantification analysis. Melting curve analysis was performed to evaluate the presence of non-specific PCR products and primer dimers. The specificity and uniqueness of the primers and the amplicons were verified by amplicon sequencing (GATC Biotech LIGHTrun). The results were exported as raw data, and the LinRegPCR[99] software was used for baseline correction. The resulting means of triplicate N_O-values, representing initial concentrations of a target and reference genes were used to analyse gene expression. For each marker, the set of qRT-PCR quantifications were standardized and rescaled to better emulate the range of RPKM values observed in the original association panel, and then predicted damage scores generated using the regression coefficient and constant from the GEM associations.

An additional GEM marker was assayed as a cSNP by PCR using 1ul undiluted cDNA, 11.5 ul Thermo Scientific Fermentas PCR Master Mix (2X), 200 nM forward (GGTTTCTCTTCTGCAGCGAG) and reverse (TCCATGATCATCTTGCTGAG) primers in a total volume of 25 µl. The touchdown PCR was performed in using a BIORAD Tetrad PCR machine with the following cycling conditions: 5 min at 94°C, followed by 15 cycles of 94°C for 30 sec, 63°C for 30 sec -1°C/cycle, 72°C for 1 min, and 30 cycles of 94°C for 30 sec, 53°C for 30 sec, 72°C for 1 min and a final elongation step at 72°C for 7 mins.

Sanger sequences obtained using the forward primer co-amplify GEM FRAEX38873_v2_000048360.1, which is highly associated with ash dieback disease damage, and another member of the gene family that is not. Due to a polymorphism between the two (at position 203 of the CDS model mentioned above), the relative abundance of the G nucleotide found in the highly associated GEM can be scored by eye relative to the A nucleotide found in the other paralog as a cSNP. Previously (Harper *et al*., 2016), this marker was scored in the Danish Test Panel as the presence or absence of a G nucleotide at this position, but predictions using this method did not incorporate the dynamic range of the gene expression observed, so for this analysis G:A peak height ratios were

approximated directly from the sequence chromatograms using Softgenetics Mutation Surveyor® software for the British Screening Panel and the Danish Test Panel. These ratios were then standardized and rescaled to the RPKM values for FRAEX38873_v2_000048360.1 in order to predict damage scores as before.

Combined predictions were made by ranking and standardizing the individual predictions for all four markers, and then calculating the mean rank score for each individual tree (Supplementary Data 6). Combined predictions were calculated for the Danish Test Panel and compared to the observed ash dieback damage scores to ensure that the assay was predictive (Fig. 3).

The four assays were applied in the same way to analyse a panel of 130 accessions originating from across the UK range of *F. excelsior* ("British Screening Panel"). Strikingly, when assayed by RT-PCR, expression of the "G" variant paralogs was seen at much higher frequency in the British Screening Panel than in the Danish panels and the mean G:A ratio across the British Screening Panel was 0.67 compared to a mean of 0.03 observed in the Danish Test Panel. Likewise, the gene expression estimates for the British Screening Panel exhibited wider ranges and were more favourable in terms of their expected effect on damage scores. The qRT-PCR results for the GEMs negatively correlated with disease damage (FRAEX38873_v2_000261470.1 and FRAEX38873_v2_000199610.1) exhibited higher mean expression in the UK (0.1±0.11 and 0.12±0.14) versus the Danish Test Panel (0.09±0.08, 0.12±0.11), and the positively correlated FRAEX38873_v2_000173540.4 was on average expressed at a lower level in the British Screening Panel (0.48±0.26) than the Danish Test Panel (0.59±0.17). As expected, this translated to lower combined predictions for ash dieback damage in the British Screening Panel. Only 9% of the Danish Test Panel accessions were predicted to have a low damage score (defined as 25% canopy damage or less) compared with 25% of the British Screening Panel (Fig. 3).

Analysis of predictive genes

In order to predict the susceptibility of the reference tree 2451S to ADB we calculated RPKM values for the five GEM marker CDS models (FRAEX38873_v2_000173540.4, FRAEX38873_v2_000048340.1, FRAEX38873_v2_000048360.1, FRAEX38873_v2_000261470.1 and FRAEX38873_v2_000199610.1) from leaf transcriptome read data. We also did this for each of the trees in the Danish Scoring Panel, and the average of these predictions taken to provide combined predictions. The top and bottom quartiles from the distribution of predicted scores, which represent the trees with the most susceptible and least susceptible gene expression patterns at these five loci, were then correlated with the RPKM values for the genome sequenced tree 2451S (Extended Data Fig. 4).

RPKM data were also generated for four tissue types: leaf, flower, cambium and root, of the parent of sequenced tree 2451S by mapping raw reads to the CDS reference as before. RPKM data for the 20 CDS models found to be significantly associated with susceptibility to ADB in the GEM analysis were selected and compared for the four tissue types.

The five CDS models represented in the ADB susceptibility predictions were translated using the standard codon usage table and were searched against the nr database in GenBank using BLASTP with default settings to identify top hits to protein sequences in *A. thaliana*: FRAEX38873_v2_000199610.1 and FRAEX38873_v2_000261470.1 show high similarity to AGAMOUS-LIKE 42/FOREVER YOUNG FLOWER (AGL42/FYF; AT5G62165); FRAEX38873_v2_000173540.4, FRAEX38873_v2_000048340.1 and FRAEX38873_v2_000048360.1 have top hits to SHORT VEGETATIVE PHASE/AGAMOUS-

LIKE 22 (SVP/AGL22; AT2G22540). Both AGL42/FYF and SVP/AGL22 are encoded by type II MADS-box genes[16]. To find potential orthologues from other species, we examined the results of the OrthoMCL analysis for clusters containing AGL42/FYF and SVP/AGL22; all sequences from these clusters were extracted and added to the appropriate *F. excelsior* sequences to create two datasets, one of AGL42/FYF-like sequences and one of SVP/AGL22-like sequences. To ensure adequate representation of putative orthologues, we further expanded these datasets to include sequences from the OrthoMCL clusters containing *A. thaliana* proteins from closely related MADS lineages, as identified by previous phylogenetic analyses of type II MADS-box sequences[16,17].

Preliminary phylogenetic analysis of these datasets revealed that, despite showing high sequence similarity in BLAST searches, FRAEX38873_v2_000048340.1 and FRAEX38873_v2_000048360.1 do not fall within the clade containing SVP/AGL22 and related *A. thaliana* sequences. Therefore, to identify potentially more closely related sequences we performed a BLASTP search of FRAEX38873_v2_000048340.1 and FRAEX38873_v2_000048360.1 against the complete set of 362,741 protein sequences used for the OrthoMCL analysis (see Supplementary Table 10), using the BLAST+ package[44] (v.2.2.31+) with an e-value cut-off of 1e-05 (FRAEX38873_v2_000048340.1 and FRAEX38873_v2_000048360.1 were not included in the OrthoMCL analysis because they were flagged as putative TE-related genes during annotation). This identified several highly similar sequences from other species with better ranking BLAST hits than those to the *A. thaliana* proteins. These sequences belong to a single OrthoMCL cluster, and include a tomato (*S. lycopersicum*) sequence from the apparent orthologue of the potato (*S. tuberosum*) *StMADS11* gene; all sequences from this cluster were added to the SVP/AGL22-like dataset, along with the potato StMADS11 protein (GenBank accession ACH53556.1).

Sequences for both datasets were aligned using M-Coffee[100], via the T-Coffee web server (www.tcoffee.org; last accessed 01.06.16) with the following parameter settings: Mpcma_msa Mmafft_msa Mclustalw_msa Mdialigntx_msa Mpoa_msa Mmuscle_msa Mprobcons_msa Mt_coffee_msa -output=score_html clustalw_aln fasta_aln score_ascii phylip -tree -maxnseq=150 -maxlen=2500 -case=upper -seqnos=on -outorder=input -run_name=result -multi_core=4 -quiet=stdout. Positions in the alignments with consensus scores of <6 from M-Coffee were removed; filtered alignments were then run through the TCS tool[101] via the T-Coffee web server and any positions with a reliability score of <6 were removed. Recombination was tested for in the filtered alignments using GARD[102]. Analyses were run via the Datamonkey server (www.datamonkey.org; last accessed 01.06.16) under the best-fit model of evolution (selected with the corrected Akaike's Information Criterion, AICc[103]) with β-Γ rate variation and three rate classes. No breakpoints with significant topological incongruence at $p \leq 0.05$ were detected for either dataset. Phylogenetic analysis of each dataset was conducted using Bayesian inference in MrBayes and maximum likelihood in RAxML; input alignments are provided in Supplementary Data 8. MrBayes (v.3.2.5[104]) was run using the mixed amino acid model, to allow models of protein sequence evolution to be fit automatically across the alignments; the following parameter settings were used for each dataset: prset aamodelpr = mixed, mcmc nruns = 2, nchains = 4, ngen = 1000000, samplefreq = 1000. Parameter values from both runs for each dataset were viewed in TRACER v1.6 (http://beast.bio.ed.ac.uk/Tracer) to confirm that effective sample sizes of >200 had been obtained for each parameter and stationarity reached. Trees sampled during the first 100000 generations of each run were discarded as the burn-in; trees and parameter values were summarised in MrBayes using the sumt and sump commands. RAxML (v.8.2.8[105]) was run using the option to automatically determine the best protein substitution model, with 1000 replicates of the rapid bootstrap algorithm; parameter settings were as follows: raxmlHPC -f a -x 13102 -p 29503 -# 1000 -m PROTGAMMAAUTO.

The phylogenetic analysis suggested that FRAEX38873_v2_000173540.4 is a likely orthologue of the *A. thaliana SVP/AGL22* gene, or possibly *AGL24*, whereas FRAEX38873_v2_000048340.1 and FRAEX38873_v2_000048360.1 appear orthologous to the potato *StMADS11* gene (Extended Data Fig. 5). These all belong to the SVP/StMADS11 group[16] of type II MADS-box genes. FRAEX38873_v2_000261470.1 and FRAEX38873_v2_000199610.1 cluster with the *A. thaliana* SUPPRESSOR of OVEREXPRESSION of CONSTANS 1(SOC1)-like proteins AGL42, AGL71 and AGL72 (Extended Data Fig. 5). The two other major clades within the phylogenetic tree include the AGL20/SOC1 protein and the AG14 and AGL19 proteins (Extended Data Fig. 5); together, the AGL42/AGL71/AGL72, AL20 and AGL14/AGL19 containing clades are known as the SOC1/TM3 group of type II MADS-box proteins[16,17].

In *A. thaliana*, *AGL42*, *AGL71* and *AGL72* have redundant functions in controlling flowering time and appear to be regulated by *AGL20*/*SOC1*[20]. In turn, *AGL20*/*SOC1* is regulated by both *AGL22/SVP* and *AGL24*[18,19], which are floral meristem identity genes with redundant functions during early stages of flower development[21]. The *StMADS11* gene does not appear to have a direct orthologue in *A. thaliana*, but in potato (*S. tuberosum*) *StMADS11* is expressed in vegetative tissues[106]. Despite their well-known roles in floral regulation, *SVP/StMADS11* and *SOC1/TM3* proteins are likely to have wider functions. In *A. thaliana*, it is suggested that *AGL22/SVP* is also required for age-related resistance (ARR), which gives older tissues of plants enhanced pathogen tolerance or resistance[24]. The *Brassica rapa BrMADS44* gene, which appears orthologous to *AGL42*, shows differential expression in response to cold and drought stress; some *B. rapa* genes belonging to the SVP/StMADS11 clade are also differentially expressed in response to these stresses, indicating a potential role in stress resistance[22]. Furthermore, many genes involved in regulation of flowering time in *A. thaliana* are involved in controlling phenology in perennial trees species and genes belonging to the SVP/StMADS11 clade have potential roles in growth cessation, bud set and dormancy[23].

Metabolomic profiling

In order to understand if trees with low and high susceptibility vary in their metabolite profiles as well as their transcriptomes, we undertook untargeted metabolite profiling on a subset of the Danish Test Panel. Untargeted metabolomics has not previously been applied to natural populations but has the potential to identify small molecules (or small molecule associations) that directly contribute to tolerance or resistance. We compared triplicate samples from five low-susceptibility Danish trees (R-14164C, R-14184A, R-14193A, R-14198B, R-14181) and five high-susceptibility trees (R-14169, R-14127, R-14156 R-14120, 25UTaps).

Three leaflets from each triplicate sample were freeze dried and gently crushed to mix tissue. Approximately 100-150mg was ground to a fine powder using a TissueLyser (Qiagen), and 10mg was extracted in 400µl 80% MeOH containing d5-IAA internal standard at 2.5ng/ml ([$^2H_5$] indole-3-acetic acid**;** OlChemIm Ltd, Czech Republic), centrifuged (10,000g, 4°C, 10 min) and the pellet re-extracted in 80% MeOH. The pooled supernatants were filtered through a 0.2µm syringe filter (Phenomenex, UK).

These leaf extracts (5 µl) were analysed using a Polaris C18 1.8 µm, 2.1 x 250 mm reverse phase analytical column (Agilent Technologies, Palo Alto, USA) and samples resolved on an Agilent 1200 series Rapid Resolution HPLC system coupled to a quadrupole time-of-flight QToF 6520 mass spectrometer (Agilent Technologies, Palo Alto, USA). Buffers were as follows: positive ion mode; mobile phase A (5% acetonitrile, 0.1% formic acid), mobile phase B (95% acetonitrile with 0.1% formic acid). Negative ion mode; mobile phase A (5%

acetonitrile with 1mM ammonium fluoride), mobile phase B (95% acetonitrile). The following gradient was used: 0 - 10 min – 0% B; 10-30 min – 0 - 100% B; 30 - 40 min – 100% B. The flow rate was 0.25 ml min^{-1} and the column temperature was held at 35 °C throughout. The source conditions for electrospray ionisation were as follows: gas temperature was 325 °C with a drying gas flow rate of 9 l min^{-1} and a nebuliser pressure of 35 psig. The capillary voltage was 3.5 kV in both positive and negative ion mode. The fragmentor voltage was 115 V and skimmer 70 V. Scanning was performed using the autoMS/MS function at 4 scans sec^{-1} for precursor ion surveying and 3 scans sec^{-1} for MS/MS with a sloped collision energy of 3.5 V/100 Da with an offset of 5 V.

Positive and negative ion data was converted into mzData using the export option in Agilent MassHunter. Peak identification and alignment was performed using the Bioconductor R package xcms[107] and features were detected using the centWave method[108] for high resolution LC/MS data in centroid mode at 30 ppm. Changes to the default parameters were: mzdiff=0.01, peakwidth=10-80, noise=1000, prefilter=3,500. Peaks were matched across samples using the density method with a bw=5 and mzwid=0.025 and retention time correlated using the obiwarp algorithm with profStep=0.5. Missing peak data was filled in the peaklists generated from the ADB low susceptibility ash leaf samples compared to the peaklists generated from the ADB susceptible leaves. The resulting peaklists were annotated using the Bioconductor R package, CAMERA[109]. The peaks were grouped using 0.05 % of the width of the full width at half maximum (FWHM) and groups correlated using a p-value of 0.05 and calculating correlation inside and across samples. Isotopes and adducts were annotated using a 10 ppm error.

Statistical analysis and modelling was performed using MetaboAnalyst v3.0 with the following parameters. Missing values were replaced using a KNN missing value estimation. Data was filtered (40%) to remove non-informative variables using the interquartile range (IQR). Samples were normalised using the internal standard d5-IAA (POS: M181T1448; NEG: M179T1382). Data was auto-scaled.

Peaks from the three replicates were aligned with xcms for both positive and negative mode and features tested for practical significance to determine the differences between the tolerant and susceptible genotypes. In addition, PLS-DA was performed using MetaboAnalyst allowing the discrimination of tolerant and susceptible genotypes based on their metabolic profiles (Fig. 4a).

The individual features (putative metabolites) that contribute to the separation between the different classes were further characterised. We first applied a range of univariate and multivariate statistical tests to determine the importance of these features. This included variable influence on the projection (VIP) values derived from PLS-DA scores, practical significance, t-test, p-value, Benjamini and Hochberg FDR (False Discovery Rate) p-value, effect size and Random Forest analysis, and MS/MS fragmentation network analysis. For example, using Random Forest, significant features were ranked by mean decrease in classification accuracy with 14/15 susceptible samples (OOB error: 0.033; class error 0.07) and 15/15 tolerant samples correctly classified.

For all further analyses we chose to use statistical and practical significance (Response screening, JMP version 12) to identify features with a practical significance for identification. A combination of k-means clustering was used to group features by patterns of abundance and also by retention time. This enabled the clustering of base peaks with their associated isotopes and adducts. Product ions were identified using MS/MS data in Agilent MassHunter Qualitative Analysis version 4.

Identification was not possible for those features with no fragmentation, or lacking significant supporting adducts. Many features of interest were identified but require further work to provide confident attributions, while some features did not provide fragmentation patterns. We thus restricted further identification and characterisation to a highly discriminatory class of compounds of the iridoid glycoside class and predominantly compounds previously recorded in Oleaceae, summarised in Extended Data Figs 6-9 and Supplementary Data 9. We validated these identifications using three methods: MS/MS fragmentation networking (Fig 4c), MS/MS mirror plot (Extended Data Figure 6) and accurate mass MS/MS product ion structure correlation (Extended Data Figure 7). The MS/MS fragmentation network was generated after extracting the m/z of the MS/MS product ions from the discriminatory features using MassHunter Qualitative Analysis Version 4 and visualized using Cytoscape indicating product ion masses which have been previously reported from fragmentation of iridoid glycosides[110]. Further validation was performed through a mirror plot comparing the MS/MS spectra of four features (N2-5) detected in negative mode with an ESI-TOF/IT-MS spectra of elenolic acid glucoside taken from the literature[112]. Finally, the accurate mass of MS/MS product ions from four discriminatory features identified in negative mode (N1-N4) were correlated with the structure of the putatively identified compound using MassHunter Molecular Structure Correlator (Agilent).

A timeline for the project may be found in Supplementary Table 14.

URLS

Genome website: www.ashgenome.org

Data availability

The reference tree is growing at Earth Trust with accession number: 2451S. Trimmed DNA and RNA reads and the final assembly for the 2451S genome sequence, as well as RNA reads for parent tree and raw reads and consensus read mappings of the European diversity panel trees have been deposited in European Nucleotide Archive (EMBL-EBI) with the project accession code "PRJEB4958" (http://www.ebi.ac.uk/ena/data/view/PRJEB4958). Metabolomic data that support the findings of this study have been deposited in MetaboLights with the accession code "MTBLS372" (www.ebi.ac.uk/metabolights/MTBLS372).

Literature Cited in Methods

31. Boshier, D. *et al. Ash species in Europe: biological characteristics and practical guidelines for sustainable use*. (Oxford Forestry Institute, University of Oxford, 2005).
32. Doyle, J. J. A rapid DNA isolation procedure for small quantities of fresh leaf tissue. *Phytochem bull* **19,** 11–15 (1987).
33. Obermayer, R., Leitch, I. J., Hanson, L. & Bennett, M. D. Nuclear DNA C□values in 30 Species Double the Familial Representation in Pteridophytes. *Ann. Bot.* **90,** 209–217 (2002).
34. Dolezel, J., Greilhuber, J. & Suda, J. Estimation of nuclear DNA content in plants using flow cytometry. *Nat. Protoc.* **2,** 2233–2244 (2007).
35. Magoč, T. & Salzberg, S. L. FLASH: fast length adjustment of short reads to improve genome assemblies. *Bioinformatics* **27,** 2957–2963 (2011).
36. Leggett, R. M., Clavijo, B. J., Clissold, L., Clark, M. D. & Caccamo, M. NextClip: an analysis and read preparation tool for Nextera Long Mate Pair libraries. *Bioinformatics* **30,** 566–568 (2014).
37. Boetzer, M., Henkel, C. V., Jansen, H. J., Butler, D. & Pirovano, W. Scaffolding pre-assembled contigs using SSPACE. *Bioinformatics* **27,** 578–579 (2011).
38. English, A. C. *et al.* Mind the gap: upgrading genomes with Pacific Biosciences RS long-read sequencing technology. *PLoS One* **7,** e47768 (2012).
39. Marçais, G. & Kingsford, C. A fast, lock-free approach for efficient parallel counting of occurrences of k-mers. *Bioinformatics* **27,** 764–770 (2011).
40. Gomez-Alvarez, V., Teal, T. K. & Schmidt, T. M. Systematic artifacts in metagenomes from complex microbial communities. *ISME J.* **3,** 1314–1317 (2009).
41. Novák, P., Neumann, P., Pech, J., Steinhaisl, J. & Macas, J. RepeatExplorer: a Galaxy-based web server for genome-wide characterization of eukaryotic repetitive elements from next-generation sequence reads. *Bioinformatics* **29,** 792–793 (2013).
42. Altschul, S. F., Gish, W., Miller, W., Myers, E. W. & Lipman, D. J. Basic local alignment

search tool. *J. Mol. Biol.* **215,** 403–410 (1990).

43. Benson, G. Tandem repeats finder: a program to analyze DNA sequences. *Nucleic Acids Res.* **27,** 573–580 (1999).

44. Camacho, C. *et al.* BLAST+: architecture and applications. *BMC Bioinformatics* **10,** 421 (2009).

45. Lamesch, P. *et al.* The *Arabidopsis* Information Resource (TAIR): improved gene annotation and new tools. *Nucleic Acids Res.* **40,** D1202–10 (2012).

46. Slater, G. S. C. & Birney, E. Automated generation of heuristics for biological sequence comparison. *BMC Bioinformatics* **6,** 31 (2005).

47. Wu, T. D. & Watanabe, C. K. GMAP: a genomic mapping and alignment program for mRNA and EST sequences. *Bioinformatics* **21,** 1859–1875 (2005).

48. Kopylova, E., Noé, L. & Touzet, H. SortMeRNA: fast and accurate filtering of ribosomal RNAs in metatranscriptomic data. *Bioinformatics* **28,** 3211–3217 (2012).

49. Trapnell, C., Pachter, L. & Salzberg, S. L. TopHat: discovering splice junctions with RNA-Seq. *Bioinformatics* **25,** 1105–1111 (2009).

50. Trapnell, C. *et al.* Transcript assembly and quantification by RNA-Seq reveals unannotated transcripts and isoform switching during cell differentiation. *Nat. Biotechnol.* **28,** 511–515 (2010).

51. Pertea, M. *et al.* StringTie enables improved reconstruction of a transcriptome from RNA-seq reads. *Nat. Biotechnol.* **33,** 290–295 (2015).

52. Haas, B. J. *et al.* De novo transcript sequence reconstruction from RNA-seq using the Trinity platform for reference generation and analysis. *Nat. Protoc.* **8,** 1494–1512 (2013).

53. Stanke, M., Steinkamp, R., Waack, S. & Morgenstern, B. AUGUSTUS: a web server for gene finding in eukaryotes. *Nucleic Acids Res.* **32,** W309–12 (2004).

54. Haas, B. J. *et al.* Automated eukaryotic gene structure annotation using EVidenceModeler and the Program to Assemble Spliced Alignments. *Genome Biol.* **9,**

1340 R7 (2008).
1341 55. Haas, B. J. *et al.* Improving the *Arabidopsis* genome annotation using maximal
1342 transcript alignment assemblies. *Nucleic Acids Res.* **31,** 5654–5666 (2003).
1343 56. Lara, A. J. *et al.* in *Innovations in Hybrid Intelligent Systems* 361–368 (Springer Berlin
1344 Heidelberg, 2007).
1345 57. Lowe, T. M. & Eddy, S. R. tRNAscan-SE: a program for improved detection of transfer
1346 RNA genes in genomic sequence. *Nucleic Acids Res.* **25,** 955–964 (1997).
1347 58. Lagesen, K. *et al.* RNAmmer: consistent and rapid annotation of ribosomal RNA genes.
1348 *Nucleic Acids Res.* **35,** 3100–3108 (2007).
1349 59. Kozomara, A. & Griffiths-Jones, S. miRBase: annotating high confidence microRNAs
1350 using deep sequencing data. *Nucleic Acids Res.* **42,** D68–73 (2014).
1351 60. Stocks, M. B. *et al.* The UEA sRNA workbench: a suite of tools for analysing and
1352 visualizing next generation sequencing microRNA and small RNA datasets.
1353 *Bioinformatics* **28,** 2059–2061 (2012).
1354 61. Lorenz, R. *et al.* ViennaRNA Package 2.0. *Algorithms Mol. Biol.* **6,** 26 (2011).
1355 62. Prüfer, K. *et al.* PatMaN: rapid alignment of short sequences to large databases.
1356 *Bioinformatics* **24,** 1530–1531 (2008).
1357 63. Muñoz-Mérida, A. *et al. De novo assembly and functional annotation of the olive (Olea*
1358 *europaea*) transcriptome. *DNA Res.* **20,** 93–108 (2013).
1359 64. Ibarra-Laclette, E. *et al.* Architecture and evolution of a minute plant genome. *Nature*
1360 **498,** 94–98 (2013).
1361 65. Denoeud, F. *et al.* The coffee genome provides insight into the convergent evolution of
1362 caffeine biosynthesis. *Science* **345,** 1181–1184 (2014).
1363 66. Jaillon, O. *et al.* The grapevine genome sequence suggests ancestral hexaploidization
1364 in major angiosperm phyla. *Nature* **449,** 463–467 (2007).
1365 67. Edgar, R. C. MUSCLE: multiple sequence alignment with high accuracy and high
1366 throughput. *Nucleic Acids Res.* **32,** 1792–1797 (2004).

68. Yang, Z. PAML 4: phylogenetic analysis by maximum likelihood. *Mol. Biol. Evol.* **24,** 1586–1591 (2007).
69. Maere, S. *et al.* Modeling gene and genome duplications in eukaryotes. *Proc. Natl. Acad. Sci. U. S. A.* **102,** 5454–5459 (2005).
70. Lyons, E., Pedersen, B., Kane, J. & Freeling, M. The Value of Nonmodel Genomes and an Example Using SynMap Within CoGe to Dissect the Hexaploidy that Predates the Rosids. *Trop. Plant Biol.* **1,** 181–190 (2008).
71. Kiełbasa, S. M., Wan, R., Sato, K., Horton, P. & Frith, M. C. Adaptive seeds tame genomic sequence comparison. *Genome Res.* **21,** 487–493 (2011).
72. Haas, B. J., Delcher, A. L., Wortman, J. R. & Salzberg, S. L. DAGchainer: a tool for mining segmental genome duplications and synteny. *Bioinformatics* **20,** 3643–3646 (2004).
73. Li, L., Stoeckert, C. J., Jr & Roos, D. S. OrthoMCL: identification of ortholog groups for eukaryotic genomes. *Genome Res.* **13,** 2178–2189 (2003).
74. Amborella Genome Project. The *Amborella* genome and the evolution of flowering plants. *Science* **342,** 1241089 (2013).
75. Kaul, S. *et al.* Analysis of the genome sequence of the flowering plant *Arabidopsis thaliana*. *Nature* **408,** 796–815 (2000).
76. Young, N. D. *et al.* The *Medicago* genome provides insight into the evolution of rhizobial symbioses. *Nature* **480,** 520–524 (2011).
77. Zimin, A. *et al.* Sequencing and assembly of the 22-gb loblolly pine genome. *Genetics* **196,** 875–890 (2014).
78. Tuskan, G. A. *et al.* The genome of black cottonwood, *Populus trichocarpa* (Torr. & Gray). *Science* **313,** 1596–1604 (2006).
79. Enright, A. J., Van Dongen, S. & Ouzounis, C. A. An efficient algorithm for large-scale detection of protein families. *Nucleic Acids Res.* **30,** 1575–1584 (2002).
80. Heberle, H., Meirelles, G. V., da Silva, F. R., Telles, G. P. & Minghim, R. InteractiVenn:

a web-based tool for the analysis of sets through Venn diagrams. *BMC Bioinformatics* **16,** 169 (2015).

81. Langmead, B. & Salzberg, S. L. Fast gapped-read alignment with Bowtie 2. *Nat. Methods* **9,** 357–359 (2012).
82. Li, H. *et al.* The Sequence Alignment/Map format and SAMtools. *Bioinformatics* **25,** 2078–2079 (2009).
83. Etherington, G. J., Ramirez-Gonzalez, R. H. & MacLean, D. bio-samtools 2: a package for analysis and visualization of sequence and alignment data with SAMtools in Ruby. *Bioinformatics* **31,** 2565–2567 (2015).
84. Cingolani, P. *et al.* A program for annotating and predicting the effects of single nucleotide polymorphisms, SnpEff: SNPs in the genome of *Drosophila melanogaster* strain w1118; iso-2; iso-3. *Fly* **6,** 80–92 (2012).
85. Ramirez-Gonzalez, R. H., Uauy, C. & Caccamo, M. PolyMarker: A fast polyploid primer design pipeline. *Bioinformatics* **31,** 2038–2039 (2015).
86. Danecek, P. *et al.* The variant call format and VCFtools. *Bioinformatics* **27,** 2156–2158 (2011).
87. Zheng, X. *et al.* A high-performance computing toolset for relatedness and principal component analysis of SNP data. *Bioinformatics* **28,** 3326–3328 (2012).
88. Hubisz, M. J., Falush, D., Stephens, M. & Pritchard, J. K. Inferring weak population structure with the assistance of sample group information. *Mol. Ecol. Resour.* **9,** 1322–1332 (2009).
89. Earl, D. A. & vonHoldt, B. M. STRUCTURE HARVESTER: a website and program for visualizing STRUCTURE output and implementing the Evanno method. *Conserv. Genet. Resour.* **4,** 359–361 (2011).
90. Jakobsson, M. & Rosenberg, N. A. CLUMPP: a cluster matching and permutation program for dealing with label switching and multimodality in analysis of population structure. *Bioinformatics* **23,** 1801–1806 (2007).

91. Buschiazzo, E., Ritland, C., Bohlmann, J. & Ritland, K. Slow but not low: genomic comparisons reveal slower evolutionary rate and higher dN/dS in conifers compared to angiosperms. *BMC Evol. Biol.* **12,** 8 (2012).
92. Barbato, M., Orozco-terWengel, P., Tapio, M. & Bruford, M. W. SNeP: a tool to estimate trends in recent effective population size trajectories using genome-wide SNP data. *Front. Genet.* **6,** 109 (2015).
93. Meglécz, E. *et al.* QDD version 3.1: a user-friendly computer program for microsatellite selection and primer design revisited: experimental validation of variables determining genotyping success rate. *Mol. Ecol. Resour.* **14,** 1302–1313 (2014).
94. Rozen, S. & Skaletsky, H. Primer3 on the WWW for general users and for biologist programmers. *Methods Mol. Biol.* **132,** 365–386 (2000).
95. Bancroft, I. *et al.* Dissecting the genome of the polyploid crop oilseed rape by transcriptome sequencing. *Nat. Biotechnol.* **29,** 762–766 (2011).
96. Popescu, A.-A., Harper, A. L., Trick, M., Bancroft, I. & Huber, K. T. A novel and fast approach for population structure inference using kernel-PCA and optimization. *Genetics* **198,** 1421–1431 (2014).
97. Zhang, Z. *et al.* Mixed linear model approach adapted for genome-wide association studies. *Nat. Genet.* **42,** 355–360 (2010).
98. Lipka, A. E. *et al.* GAPIT: genome association and prediction integrated tool. *Bioinformatics* **28,** 2397–2399 (2012).
99. Ruijter, J. M. *et al.* Amplification efficiency: linking baseline and bias in the analysis of quantitative PCR data. *Nucleic Acids Res.* **37,** e45 (2009).
100. Di Tommaso, P. *et al.* T-Coffee: a web server for the multiple sequence alignment of protein and RNA sequences using structural information and homology extension. *Nucleic Acids Res.* **39,** W13–7 (2011).
101. Chang, J.-M., Di Tommaso, P. & Notredame, C. TCS: a new multiple sequence alignment reliability measure to estimate alignment accuracy and improve phylogenetic

tree reconstruction. *Mol. Biol. Evol.* **31,** 1625–1637 (2014).

102. Kosakovsky Pond, S. L., Posada, D., Gravenor, M. B., Woelk, C. H. & Frost, S. D. W. GARD: a genetic algorithm for recombination detection. *Bioinformatics* **22,** 3096–3098 (2006).

103. Sugiura, N. Further analysts of the data by akaike's information criterion and the finite corrections: Further analysts of the data by akaike's. *Communications in Statistics-Theory and Methods* **7,** 13–26 (1978).

104. Ronquist, F. *et al.* MrBayes 3.2: efficient Bayesian phylogenetic inference and model choice across a large model space. *Syst. Biol.* **61,** 539–542 (2012).

105. Stamatakis, A. RAxML version 8: a tool for phylogenetic analysis and post-analysis of large phylogenies. *Bioinformatics* **30,** 1312–1313 (2014).

106. Carmona, M. J., Ortega, N. & Garcia-Maroto, F. Isolation and molecular characterization of a new vegetative MADS-box gene from *Solanum tuberosum* L. *Planta* **207,** 181–188 (1998).

107. Smith, C. A., Want, E. J., O'Maille, G., Abagyan, R. & Siuzdak, G. XCMS: processing mass spectrometry data for metabolite profiling using nonlinear peak alignment, matching, and identification. *Anal. Chem.* **78,** 779–787 (2006).

108. Tautenhahn, R., Böttcher, C. & Neumann, S. Highly sensitive feature detection for high resolution LC/MS. *BMC Bioinformatics* **9,** 504 (2008).

109. Kuhl, C., Tautenhahn, R., Böttcher, C., Larson, T. R. & Neumann, S. CAMERA: an integrated strategy for compound spectra extraction and annotation of liquid chromatography/mass spectrometry data sets. *Anal. Chem.* **84,** 283–289 (2012).

110. Li, C.-M. *et al.* Structural characterization of iridoid glucosides by ultra-performance liquid chromatography/electrospray ionization quadrupole time-of-flight tandem mass spectrometry. *Rapid Commun. Mass Spectrom.* **22,** 1941–1954 (2008).

111. Wicker, T. *et al.* A unified classification system for eukaryotic transposable elements. *Nat. Rev. Genet.* **8,** 973–982 (2007).

1475 112. Gupta, S. D. *Reactive oxygen species and antioxidants in higher plants*. (CRC Press,
1476 2010).

Acknowledgments

Eurofins MWG GmbH provided a discounted service for Illumina and 454 sequencing of the reference genome, funded by NERC Urgency Grant, NE/K01112X/1 to R.J.A.B.. The associative transcriptomic and metabolomic work was part of the the “Nornex” project led by J.A.D. funded jointly by UK BBSRC (BBS/E/J/000CA5323) and DEFRA. The Genome Analysis Centre, Norwich, UK sequenced the European diversity panel, funded by the “Nornex” project and a National Capability in Genomics (BB/J010375/1) grant. William Crowther (Queen Mary University of London) assisted with DNA extractions for the KASP assay; The John Innes Centre contributed KASP analyses. Juliana Fabiana Miranda assisted with RNA extractions and qRT-PCR at University of York. Dr Hannah Florance, Prof. Nicholas Smirnoff and the Exeter Metabolomics Facility developed metabolomic methods and ran samples, and Dr Tom Howard for helped with statistics. L.J.K and R.J.A.B. were partly funded by LWEC Tree Health and Plant Biosecurity Initiative - Phase 2 Grant, BB/L012162/1 to R.J.A.B., S.L. and Paul Jepson (University of Oxford) funded jointly by a grant from BBSRC, Defra, ESRC, the Forestry Commission, NERC and the Scottish Government, under the Tree Health and Plant Biosecurity Initiative. G.W. was funded by Teagasc Walsh Fellowship 2014001 to R.J.A.B. and G. C. D.. E.D.C was funded by Marie Skłodowska-Curie Individual Fellowship “FraxiFam” (grant agreement 660003) to E.D.C. and R.J.A.B. E.S.A.S. and J.Z. are funded by the Marie-Curie Initial Training Network INTERCROSSING. R.H.R.G. is supported by a Norwich Research Park PhD Studentship and The Genome Analysis Centre Funding and Maintenance Grant. This research utilised Queen Mary's MidPlus computational facilities, supported by QMUL Research-IT and funded by EPSRC grant EP/K000128/1 and NERC EOS Cloud.

Author information

These authors contributed equally to this work
Elizabeth SA Sollars, Andrea L Harper, Laura J Kelly, Christine Sambles

Affiliations

School of Biological and Chemical Sciences, Queen Mary University of London, Mile End Road, London E1 4NS, UK
Elizabeth SA Sollars, Laura J Kelly, Gemma Worswick, Jasmin Zohren, Endymion D Cooper, Richard JA Buggs

QIAGEN Aarhus A/S, Silkeborgvej 2, Prismet, 8000 Aarhus C., Denmark
Elizabeth SA Sollars

Royal Botanic Gardens Kew, Richmond, Surrey, TW9 3AB, UK
Richard JA Buggs

Centre for Novel Agricultural Products, University of York, Heslington, York, YO10 5DD, UK
Andrea L Harper, Lenka Havlickova, Yi Li, Zhesi He, Alison Fellgett, Ian Bancroft

The Genome Analysis Centre, Norwich Research Park, Norwich, NR4 7UH, UK
Ricardo Ramirez-Gonzalez, David Swarbreck, Gemy Kaithakottil, Mario Caccamo

Biosciences, College of Life and Environmental Sciences, University of Exeter, Exeter, UK
Christine Sambles, David J Studholme, Deborah L. Salmon, Murray Grant

School of life Sciences, Gibbet Hill Campus, University of Warwick, Coventry, UK
Murray Grant (Present address)

Earth Trust, Little Wittenham, Abingdon, Oxfordshire, OX14 4QZ, UK
Jo Clark

Department of Plant Sciences, University of Oxford, OX1 3RB, UK
David Boshier

Forest Research, Northern Research Station, Roslin, Midlothian, EH25 9SY, UK
Steve Lee

Department of Geosciences and Natural Resource Management, University of Copenhagen, Denmark
Lea Vig McKinney, Lene Rostgaard Nielsen, Erik Dahl Kjær

Teagasc, Agriculture and Food Development Authority, Ashtown, Dublin, D15 KN3K, Ireland

Gerry C Douglas

John Innes Centre, Norwich Research Park, NR4 7UH, UK
Cristobal Uauy, J. Allan Downie

National Institute of Agricultural Botany, Cambridge, CB3 0LE, UK
Mario Caccamo

The *F. excelsior* 2451S genome sequence and final assembly, as well as RNA reads for parent tree and raw reads and consensus read mappings of the European diversity panel trees were submitted to European Nucleotide Archive (EMBL-EBI) under project accession PRJEB4958.

Author Contributions

R.J.A.B, M.C., D.S., M.G., J.A.D. and I.B. are the lead investigators. R.J.A.B. coordinated the project and directed work on the reference genome. E.S.A.S. assembled the reference genome and organellar genomes, and analysed: gene and genome duplications, European population structure, past effective population sizes. L.J.K. extracted HMW DNA for the European diversity panel and conducted repetitive element, OrthoMCL and phylogenetic analyses. G.W. conducted SSR analyses. J.Z. extracted HMW DNA and RNA for the reference genome, E.D.C. analysed genome duplication in the reference genome. D.S. and G.K. carried out bioinformatic analyses to annotate the reference genome. M.C. conceived of and, with R.J.A.B., oversaw the European-wide diversity panel sequencing. R.R.-G., E.S.A.S. and M.C. carried out SNP calling on the European-wide diversity panel, and KASP genotyping. C.U. conducted KASP genotyping. B.J.C. conceived of and oversaw the NEXTERA sequencing on the reference tree genome. M.C., J.A.D. and B.J.C. generated the first-pass “Tree 35” Illumina reads included in the European-wide SNP analysis. E.D.K., L.R.N. and L.V.M., generated, selected and collected Danish samples. D.B. generated and J.C. maintained and sampled the reference tree. J.C., D.B, G. C. D. and S.L. generated, selected and collected U.K. and European-wide diversity panel samples.
For the associative transcriptomics: I.B and A.L.H. conceived and planned the study; A.L.H., L.H., and A.F. performed experiments; bioinformatics was executed by Y.L. and Z.H and A.L.H. completed the data analysis. For the metabolomics: C.S., D.J.S., and M.G. conceived and conducted the analyses; C.S. developed methodology, and D.L.S. processed and extracted samples and ran the mass-spectrometer.

Competing financial interests

The authors declare no competing financial interests.

Corresponding author

Correspondence to Richard Buggs <r.buggs@qmul.ac.uk>

Extended Data Figure Legends

Extended Data Figure 1 | Completeness and coherence of annotation models. a, Assessment of transcript completeness for the *F. excelsior* gene set. Transcripts were classified as full-length, 5'- end, 3'-end, internal, coding (ORF predicted but no blast support), unknown (no blast support), mis-assembled and putative ncRNA using Full-lengtherNEXT (v0.0.8), 76.43% of transcript models were identified as complete.**b,** Coherence in gene length between *F. excelsior* and *M. guttatus* proteins. Blast analysis (1e-5) identified 2,576 proteins that had reciprocal best hits to 2,605 *Mimulus guttatus* proteins identified as single copy in *Mimulus guttatus, Solanum lycopersicum, Solanum tuberosum* and *Vitis vinifera* (Phytozome). A high coherence in gene length was found between *Fraxinus excelsior* and *Mimulus guttatus r* > 0.917.

Extended Data Figure 2 | Synteny between ash and monkey flower. Syntenic dotplot between ash (vertical axis) and monkey flower (horizontal axis) showing regions of multiple synteny. Scaffolds equal to approximately 75% of the ash genome assembly for which syntenic blocks were not detected are not shown. For clarity small scaffold names are omitted.

Extended Data Figure 3 | Population structure of *F. excelsior* in Europe. a, Results from STRUCTURE; three replicates were run for k=3, with each replicate using a different set of 8,955 SNPs as input. Numbers refer to samples, whose locations are given in Supplementary Table 11. **b,** Delta K values for three runs of STRUCTURE of each value of k between k=2 and k=19. k=3 has the highest Delta K value of 32.91. **c,** Effective population size history estimated using the SNeP program, with genotype information from all 38 diversity panel samples at 394,885 SNP loci.

Extended Data Figure 4 | Prediction of susceptibility of reference tree. RPKM values for leaf material from the low heterozygosity reference tree 2451S for 5 CDS models predictive for ADB. These are shown next to expression profiles for the Danish Scoring Panel with the least susceptible and most susceptible expression patterns according to the GEM analysis.

Extended Data Figure 5 | Investigation of the function of GEM markers for low susceptibility to ash dieback. Unrooted maximum likelihood (ML) trees from the RAxML analyses. **a,** Best scoring ML tree from the phylogenetic analysis of SVP/AGL22 and StMADS11-like sequences. **b,** Best scoring ML tree for the SOC1-like sequences. Nodes with bootstrap support values of ≥70 from the ML analysis and posterior probabilities of ≥0.95 from the Bayesian analysis are indicated with asterisks. *Fraxinus excelsior* sequences are shown in blue; *A. thaliana* sequences in red. Four-letter taxon codes at the start of sequence names, where present, follow those in Extended Data Table 1. Sequence names are those from the original data files used for the orthoMCL analysis (see Supplementary Table 10), with the exception of the StMADS11 protein from potato, where the GenBank accession number is given. Common names for selected genes/proteins are annotated on the trees. Scale bars indicate the mean number of substitutions per site.

Extended Data Figure 6 | MS-MS Mirror plot of elenolic acid glucoside (ESI-TOF/IT-MS) compared to four negative mode features (N2, N3, N4 and N5). The spectra share four product ions in common, m/z 179, 223, 371 and 403 (elenolic acid glucoside molecular ion). These product ions correspond to a loss of a methyl and hydroxyl group (403-371), loss of hexose (403-223) which is followed by a loss of CO_2 (223-179). Elenolic acid corresponds to the secoiridoid part of oleuropein-related compounds suggesting that these four compounds are secoiridoids[112].

Extended Data Figure 7 | Identification of MS-MS product ions for four iridoid glycoside related features observed in negative mode. Predicted structure for key m/z peaks using Molecular Structure Correlator (Agilent) and the structure of putative IDs. Bonds and atoms in black are present in that product ion, whereas gray indicates loss.

Extended Data Figure 8 | Identification of iridoid glycoside related metabolites in positive mode. Box plots showing abundance (log2 transformed) of features in positive mode discriminating between 5 different genotypes of high (TOL) and low (SUS) susceptibility ash trees.

Extended Data Figure 9 | Identification of metabolites. MS/MS fragmentation product ion data of features discriminating between five different genotypes of high (TOL) and low (SUS) susceptibility ash trees in positive mode. Corresponding box-plots are presented in Extended Data Fig. 8.

Extended Data Table Legend

Extended Data Table 1 | The 20 largest clusters in *Fraxinus excelsior* from the OrthoMCL analysis of 11 species, showing the number of sequences from each species belonging to the clusters. Clusters containing at least five more sequences from *F. excelsior* than for the other Asterid species (underlined) are shown in bold. FEXC = *Fraxinus excelsior*; ATHA = *Arabidopsis thaliana*; ATRI = *Amborella trichopoda*; CCAN = *Coffea canephora*; MGUT = *Mimulus guttatus*; MTRU = *Medicago truncatula*; PITA = *Pinus taeda*; PTRI = *Populus trichocarpa*; SLYC = *Solanum lycopersicum*; UGIB = *Utricularia gibba*; VVIN = *Vitis vinifera*. Details of gene families in column two are inferred from the gene family membership/function of *A. thaliana* genes (according to The Arabidopsis Information Resource; www.arabidopsis.org) belonging to these clusters. It should be noted that OrthoMCL clusters are not necessarily equivalent to gene families as a single gene family may be split over multiple clusters and multiple gene families may be grouped into a single cluster.

a

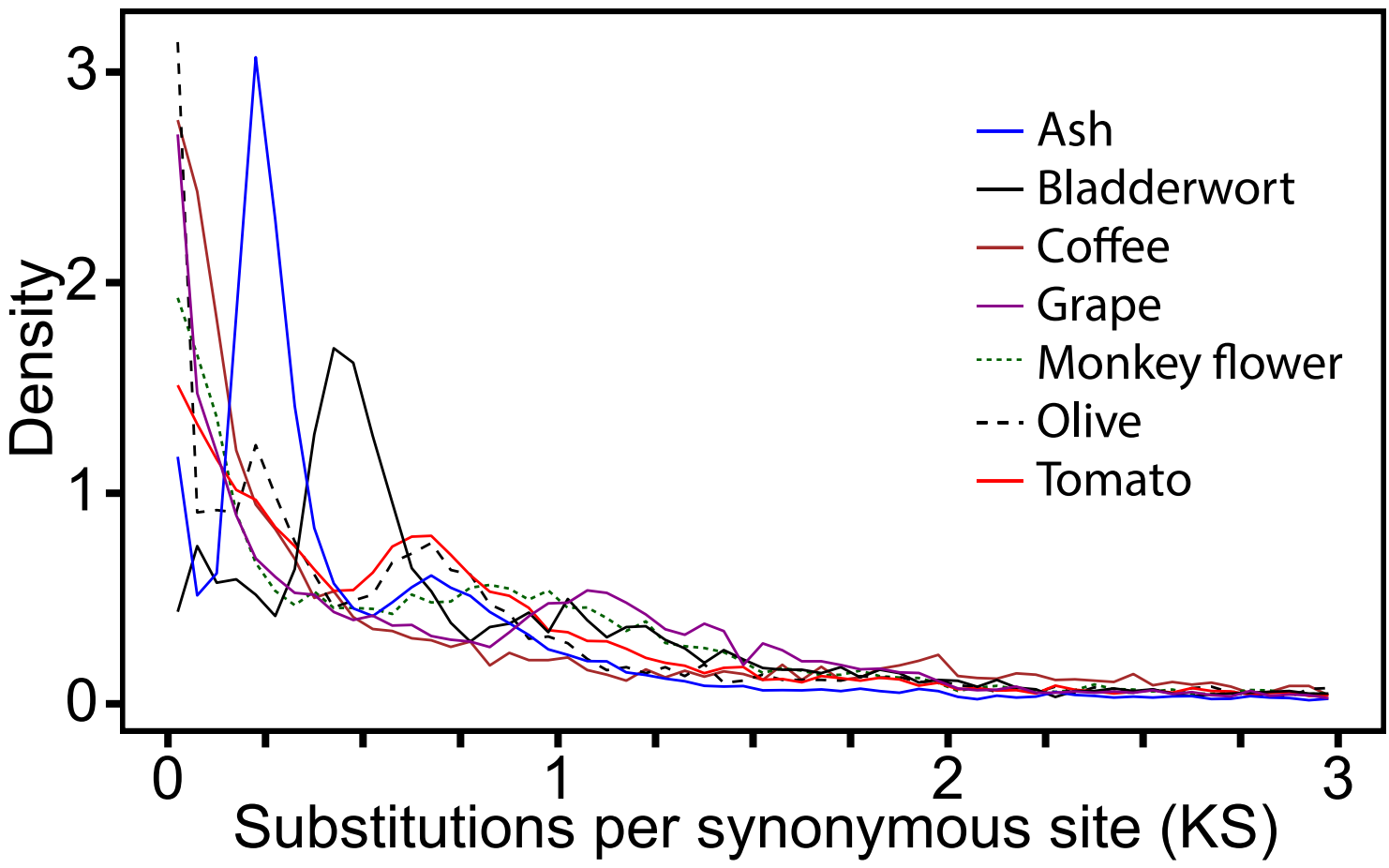
Density
Substitutions per synonymous site (KS)
Ash
Bladderwort
Coffee
Grape
Monkey flower
Olive
Tomato

b

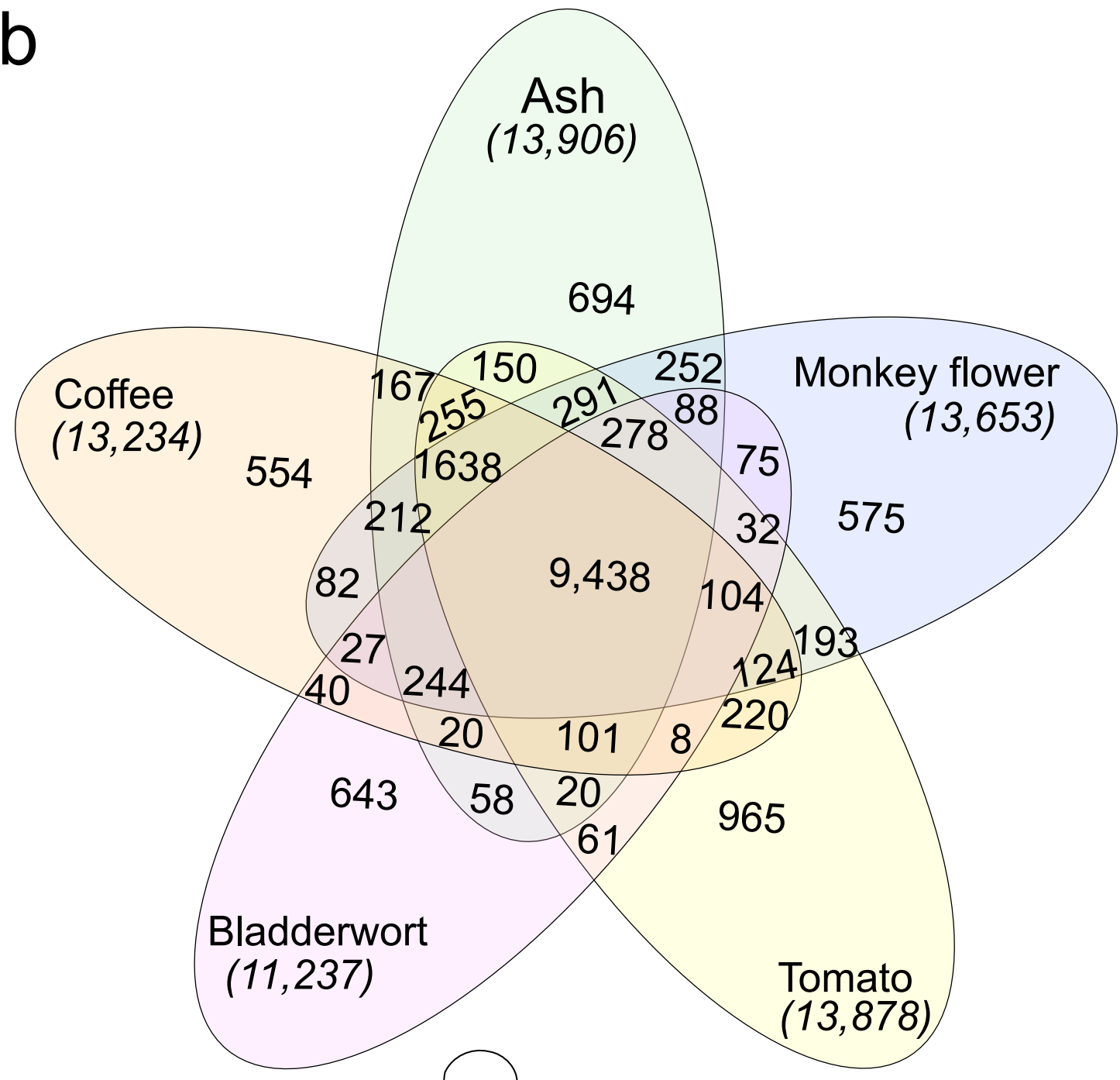
Ash
(13,906)
694
Coffee
(13,234)
554
Monkey flower
(13,653)
575
Bladderwort
(11,237)
643
Tomato
(13,878)
965
167
150
252
255
291
88
278
75
1638
212
32
82
9,438
104
27
244
193
124
40
20
101
8
220
58
20
61

c

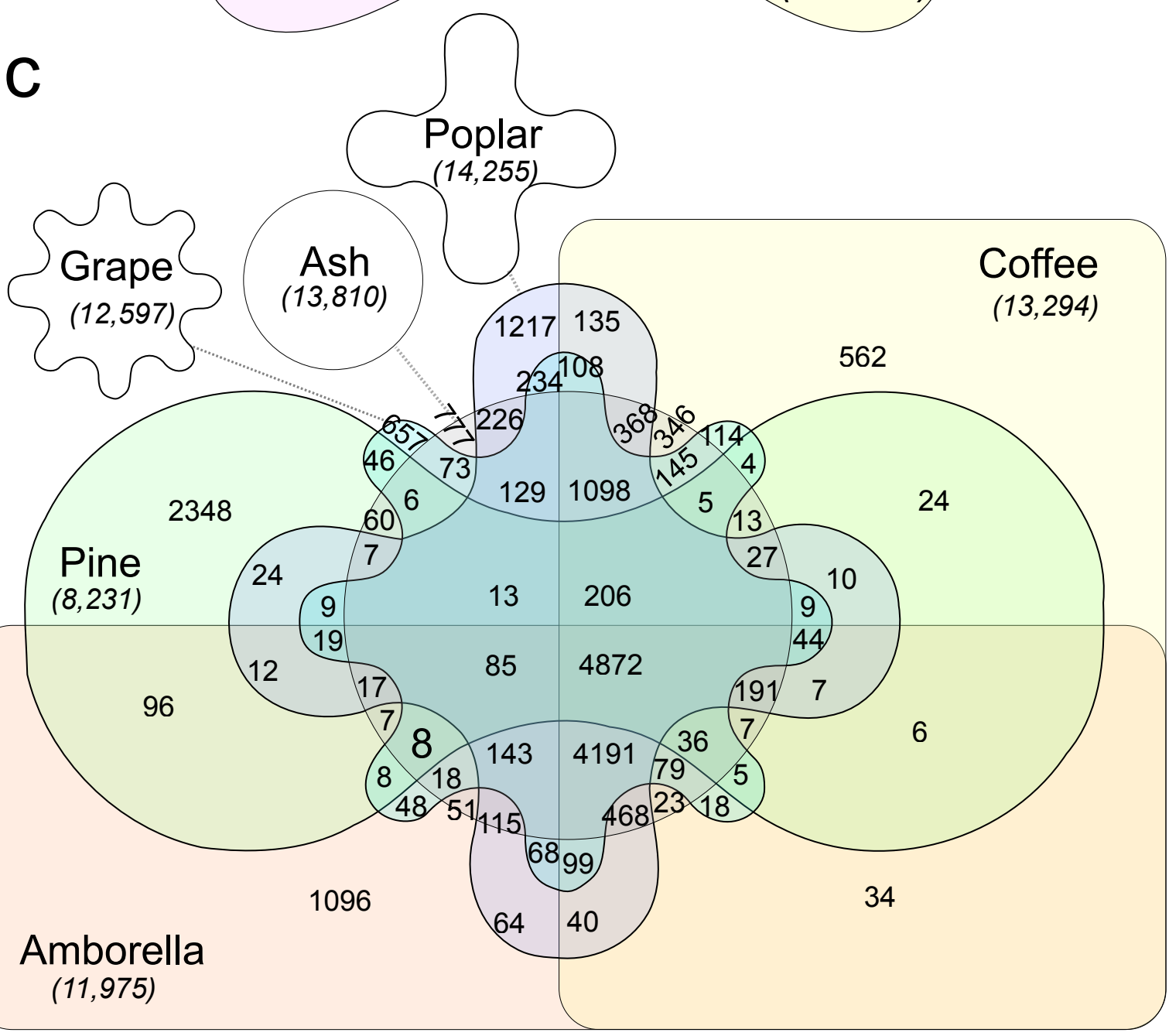
Poplar
(14,255)
Grape
(12,597)
Ash
(13,810)
Coffee
(13,294)
Pine
(8,231)
Amborella
(11,975)
2348
562
24
96
6
1096
34
1217
135
108
234
657
226
368
346
114
46
73
145
4
6
129
1098
5
13
60
7
27
24
10
9
13
206
9
19
44
12
85
4872
17
191
7
7
8
143
4191
36
7
79
5
8
18
48
51
115
468
23
18
68
99
64
40

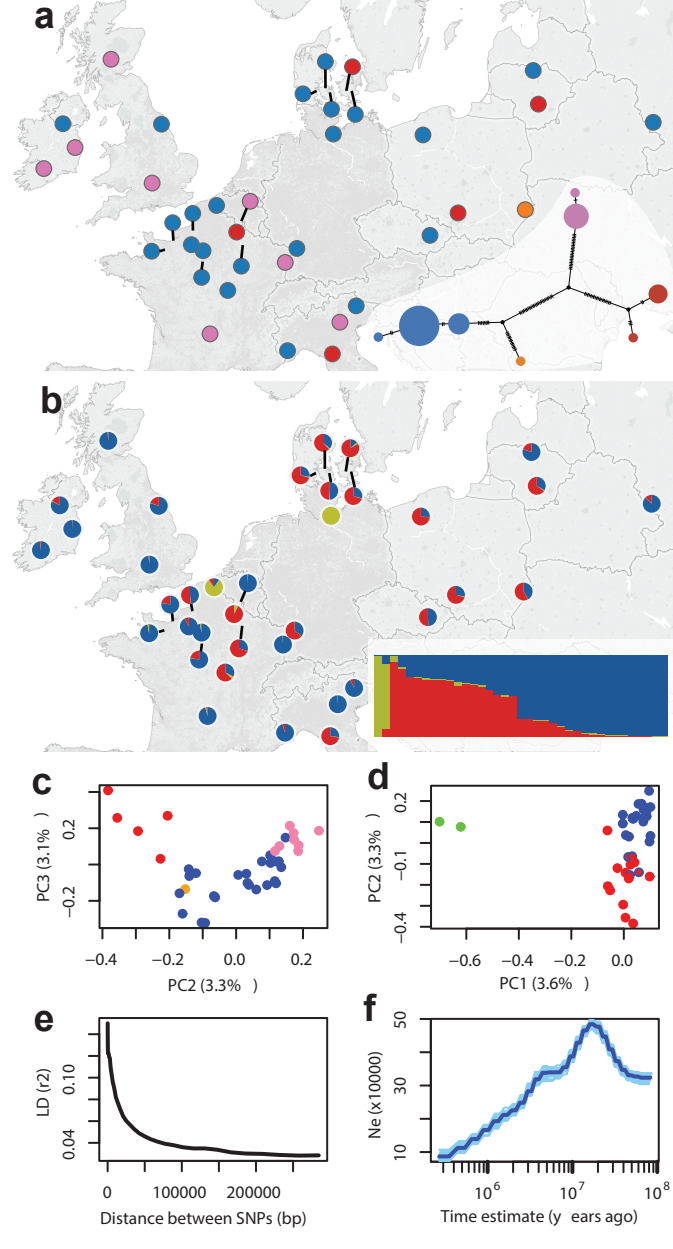
a
b
c
PC3 (3.1%)
0.2
−0.2
−0.4
−0.2
0.0
0.2
PC2 (3.3%)
d
PC2 (3.3%)
0.2
−0.1
−0.4
−0.6
−0.4
−0.2
0.0
PC1 (3.6%)
e
LD (r2)
0.10
0.04
0
100000
200000
Distance between SNPs (bp)
f
Ne (x10000)
50
30
10
10^6
10^7
10^8
Time estimate (y ears ago)

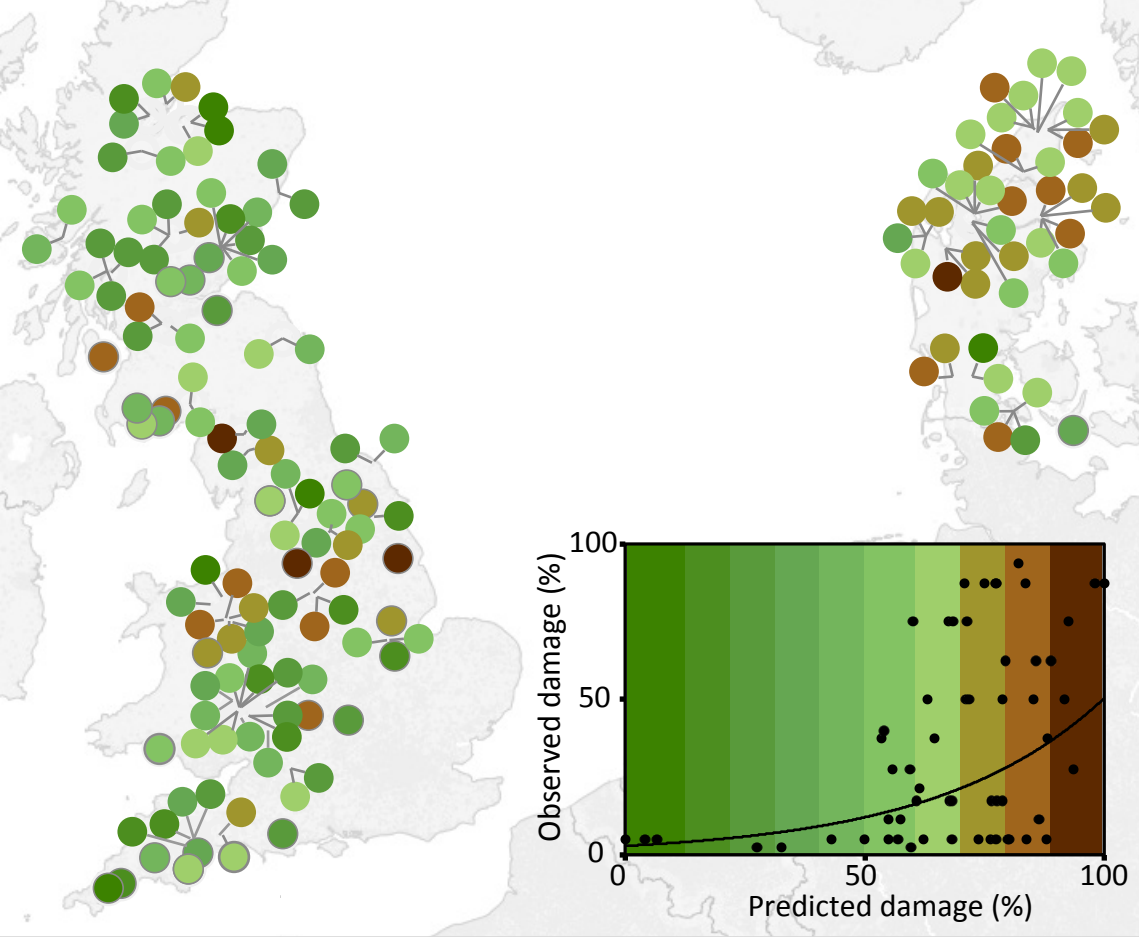
100
50
0
Observed damage (%)
0
50
100
Predicted damage (%)

a

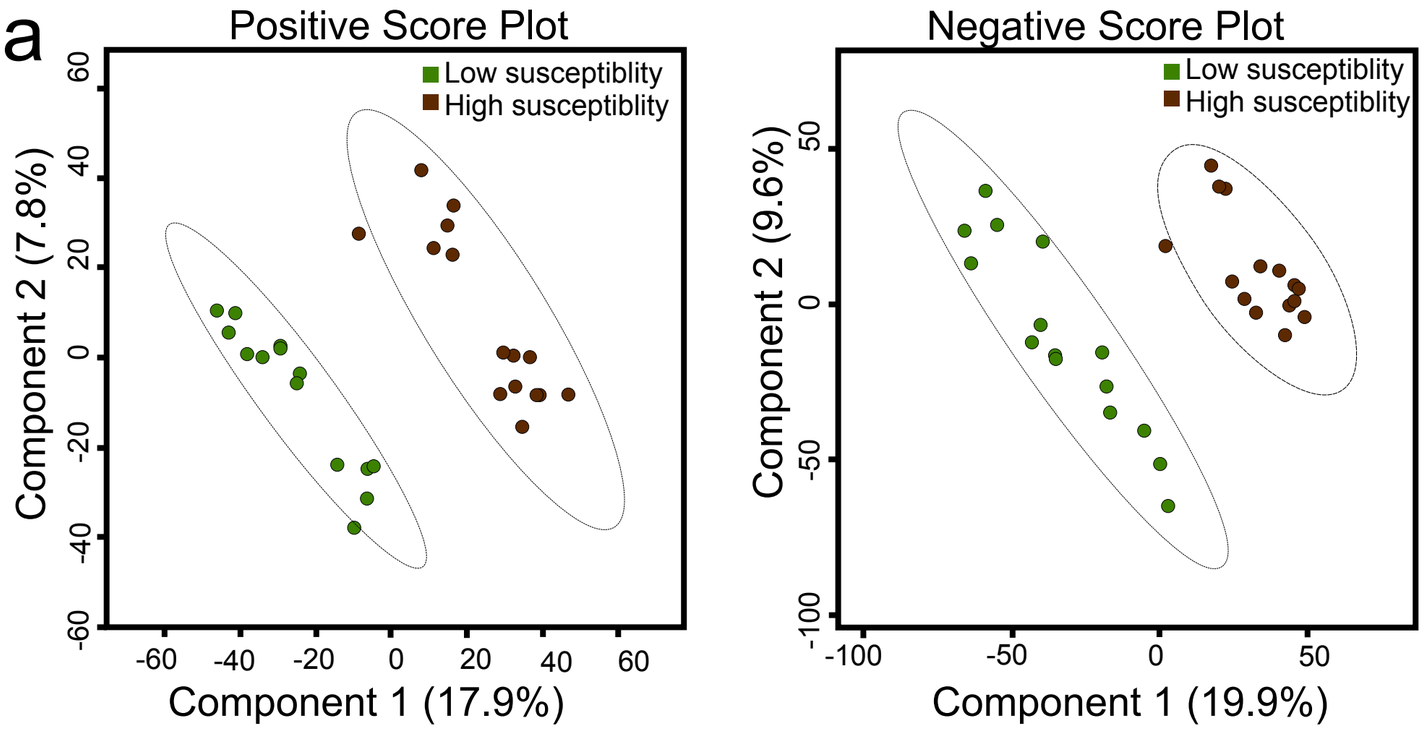
Positive Score Plot
Low susceptiblity
High susceptiblity
Component 2 (7.8%)
Component 1 (17.9%)
Negative Score Plot
Low susceptiblity
High susceptiblity
Component 2 (9.6%)
Component 1 (19.9%)

b

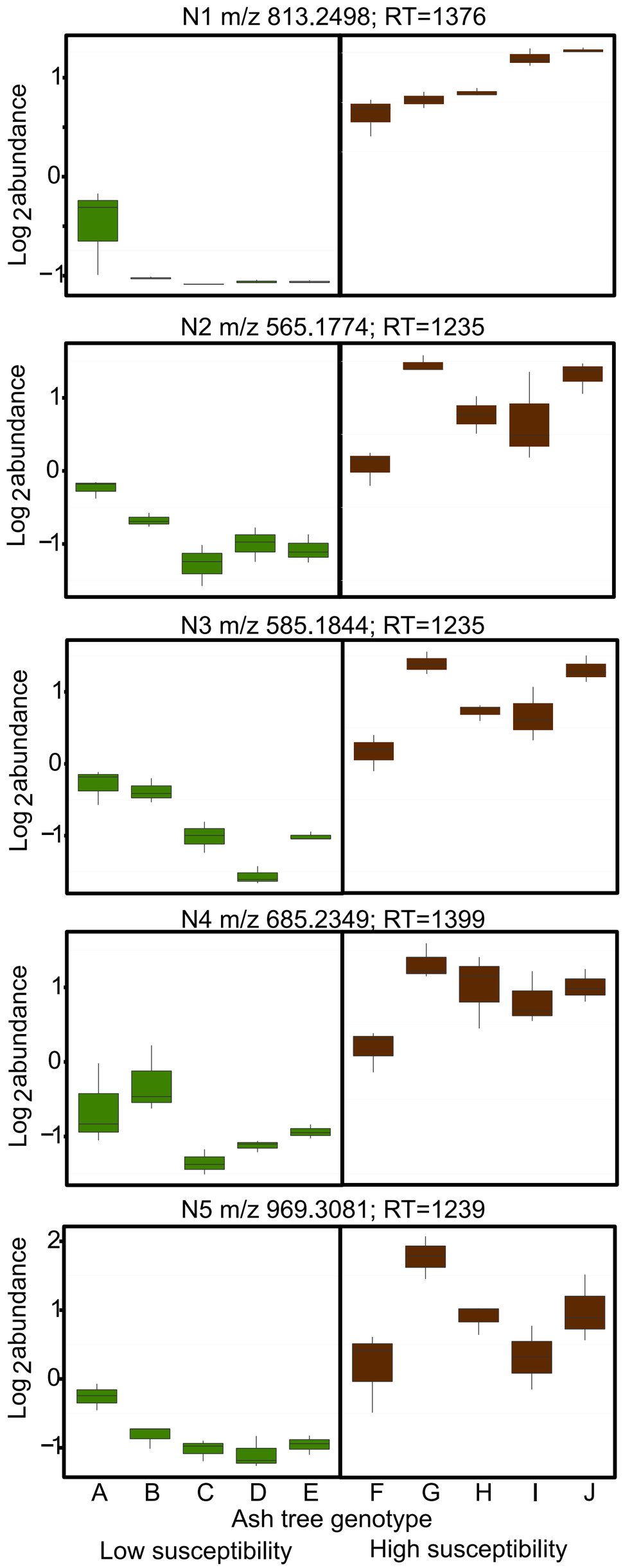
N1 m/z 813.2498; RT=1376
N2 m/z 565.1774; RT=1235
N3 m/z 585.1844; RT=1235
N4 m/z 685.2349; RT=1399
N5 m/z 969.3081; RT=1239
Log 2abundance
A
B
C
D
E
F
G
H
I
J
Ash tree genotype
Low susceptibility
High susceptibility

c

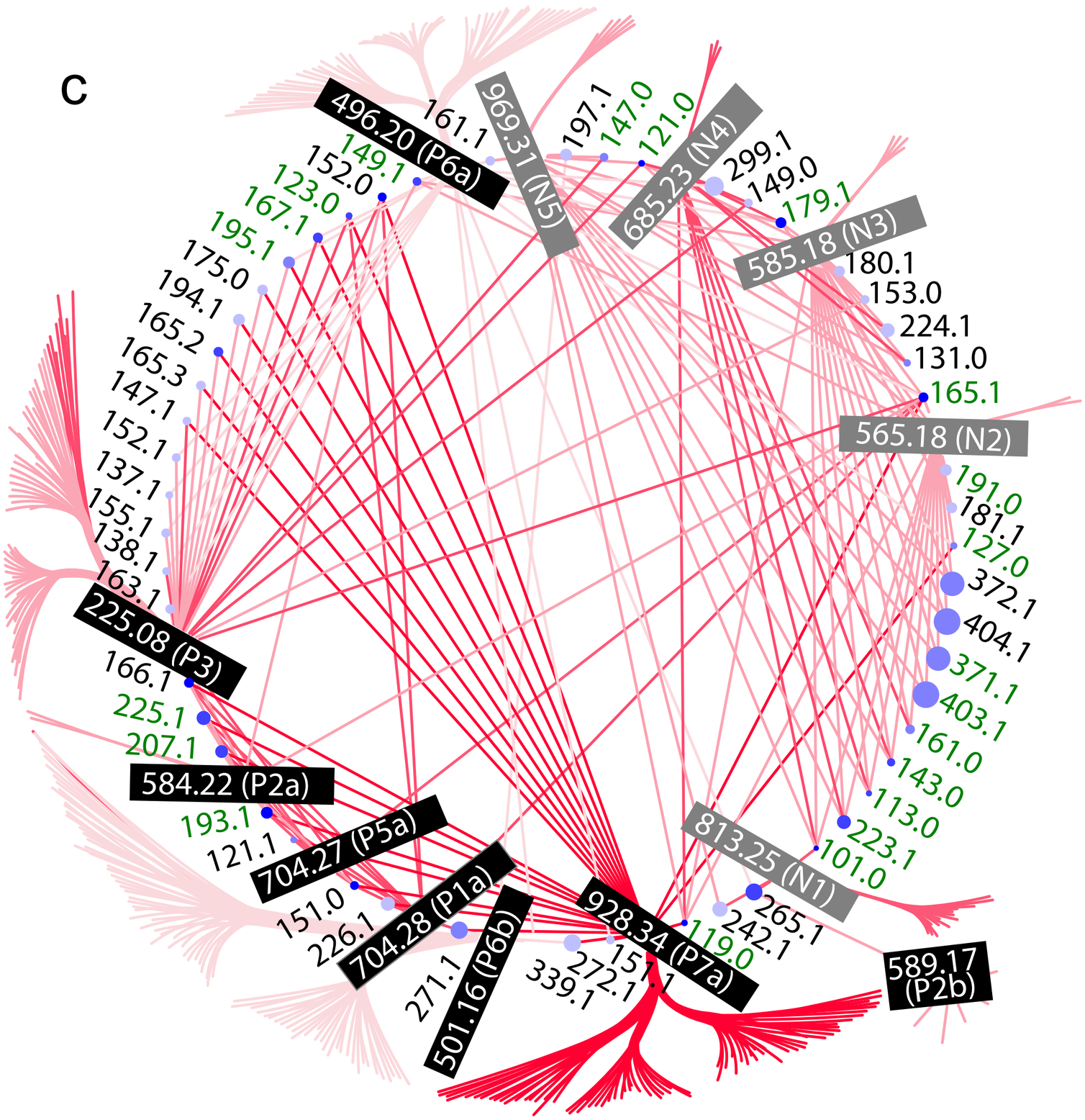
496.20 (P6a)
969.31 (N5)
685.23 (N4)
585.18 (N3)
565.18 (N2)
813.25 (N1)
928.34 (P7a)
704.28 (P1a)
704.27 (P5a)
584.22 (P2a)
225.08 (P3)
501.16 (P6b)
589.17 (P2b)